haematologica
Journal of the Ferrata Storti Foundation

Interleukin signaling mitigates the inhibitory effects of combined Src/BCR-ABL blockade on T-cell activity in Philadelphia chromosome-positive acute lymphoblastic leukemia

by Farnaz Naeemikia, Joshua Reynolds, Cheng Dong and Justin R. Pritchard

Received: August 4, 2025.
Accepted: January 16, 2026.

Citation: Farnaz Naeemikia, Joshua Reynolds, Cheng Dong and Justin R. Pritchard. Interleukin signaling mitigates the inhibitory effects of combined Src/BCR-ABL blockade on T-cell activity in Philadelphia chromosome-positive acute lymphoblastic leukemia.
Haematologica. 2026 Feb 5. doi: 10.3324/haematol.2025.288829 [Epub ahead of print]

Interleukin signaling mitigates the inhibitory effects of combined Src/BCR-ABL1 blockade on T-cell activity in Philadelphia chromosome-positive acute lymphoblastic leukemia

Farnaz Naeemikia [1], Joshua Reynolds [1], Cheng Dong [1], Justin R Pritchard* [1,2]

[1] Department of Biomedical Engineering, University Park, The Pennsylvania State University, PA, United States

[2] Huck Institute for the Life Sciences, University Park, The Pennsylvania State University, PA, United States

*Correspondence: Justin R. Pritchard Jrp94@psu.edu

Author Disclosures: JRP has consulted for Takeda Pharmaceuticals, Versant Ventures, Von Pfeffel Pharmaceuticals, Atlas Biotech, Curie.Bio, Galapagos NV, MOMA Therapeutics, Red Ace Bio, F. Hoffman La Roche, Genentech, Theseus Pharmaceuticals, WuXi Next Code and Third Rock Ventures. JRP has received travel funding from Roche, Genentech, Theseus and MOMA Therapeutics. JRP has received equity in Red Ace Bio, MOMA Therapeutics and Theseus Pharmaceuticals.

Author Contributions: JRP supervised the project, provided funding, designed experiments and data analysis and interpretation, developed analytical methods, and wrote the manuscript; **FN** designed and performed experiments, data analysis and interpretation, developed and implemented MATLAB MCMC code (Numerical methods), and wrote the manuscript, **JAR** performed, optimized experiments and analyzed data. **CD** provided funding, project supervision.

Data Sharing Statement:

The custom code and scripts used for data analysis and visualization in this study are available from the corresponding author upon reasonable request. MATLAB Code is available at https://zenodo.org/badge/DOI/10.5281/zenodo.16540528.svg (MCMC code-T cell and B cell interaction).

Funding

Research reported in this publication was supported by the National Center for Advancing Translational Sciences of the National Institutes of Health Award Number TL1TR002016 and 5TL1TR002016-06 and U01CA265709. The content is solely the responsibility of the authors and does not necessarily represent the official views of the NIH.

Abstract

Philadelphia chromosome-positive acute lymphoblastic leukemia (Ph+ ALL), driven by the BCR-ABL1 fusion gene, remains a high-risk malignancy despite therapeutic advances. Tyrosine kinase inhibitors (TKIs) targeting BCR-ABL1 have significantly improved outcomes, but resistance and relapse persist, necessitating novel strategies such as combining TKIs with bispecific T-cell engagers (BiTEs) like blinatumomab. Blinatumomab redirects T cells to eliminate CD19+ leukemia cells and has shown impressive clinical activity in Ph+ ALL when combined with Src+BCR-ABL1 TKIs. However, this contrasts with preclinical observations reporting that Src kinase inhibition by Src/BCR-ABL1 TKIs antagonizes blinatumomab-mediated T-cell activation. Consistent with prior preclinical studies, we demonstrate that dasatinib and ponatinib, unlike SRC sparing TKIs (imatinib, nilotinib), antagonize blinatumomab's T-cell engaging efficacy by potently inhibiting LCK Y394 phosphorylation, a critical step in proximal TCR signaling. This inhibition impairs T-cell proliferation, cytokine production, and NFAT activation. To reconcile this *in vitro* antagonism with favorable clinical combination outcomes, we confirmed that the mechanism of SRC inhibition is T-cell intrinsic and explored the impact of interleukins. We show that TKI-induced T-cell suppression and antagonism can be significantly improved by supplementing co-cultures with common gamma-chain cytokines, particularly IL-7. IL-7 robustly enhances human T-cell proliferation, reduces exhaustion, and significantly improves blinatumomab's cytotoxic efficacy in the presence of Src/BCR-ABL1 TKIs.

Introduction

Philadelphia chromosome-positive acute lymphoblastic leukemia (Ph+ ALL) is an aggressive subtype of B-cell precursor ALL, accounting for approximately 25-30% of adult cases.[1,2] This malignancy is driven by the t(9;22)(q34;q11) translocation, generating the BCR-ABL1 fusion gene, which encodes a constitutively active tyrosine kinase. Historically, Ph+ ALL carried a poor prognosis, with limited response to conventional chemotherapy and low long-term survival rates [3,4].

The introduction of tyrosine kinase inhibitors (TKIs) targeting BCR-ABL1 markedly improved outcomes. First-generation TKIs like imatinib showed promise but were limited by resistance, often due to BCR-ABL kinase domain mutations[5,6]. Second- and third-generation TKIs, including dasatinib, nilotinib, and ponatinib, were developed to overcome these mutations, particularly the T315I "gatekeeper" mutation[7]. Ponatinib plus chemotherapy is now the standard of care, as demonstrated in the Phase 3 PhALLCON study, which showed a significantly higher rate of MRD-negative remission compared to imatinib (34.4% vs. 16.7%)[8,9].

Despite progress, durable remission remains a challenge, necessitating novel approaches. Bispecific T-cell engagers (BiTEs), such as blinatumomab, redirect T cells to lyse CD19+ B cells and have shown efficacy in relapsed/refractory B-cell precursor ALL[10]. Blinatumomab is now being explored in chemotherapy-free regimens with TKIs, demonstrating encouraging clinical outcomes[11].

TKI-BiTE combinations have yielded remarkable rates of MRD negativity and improved survival[12]. For instance, a study combining dasatinib and blinatumomab showed an overall survival (OS) rate of 80.7% at 53 months [13,14] A separate phase II trial of blinatumomab and ponatinib reported a 3-year OS rate of 88% and 98% of patients achieving MRD negativity.[15] These high rates of durable remission underscore the transformative potential of chemotherapy-free combinations for long-term disease control in Ph+ ALL[16].

However, the combination of blinatumomab with potent Src family kinase (SFK) inhibitors like dasatinib and ponatinib presents a potential mechanistic conflict[17]. LCK and FYN are pivotal tyrosine kinases in the T-cell receptor (TCR) signaling pathway, and are essential for T-cell activation, proliferation, and effector function[18]. Previous *in vitro* studies have suggested that these TKIs can impair T-cell activation and blinatumomab-mediated cytotoxicity by inhibiting LCK activity[19,20]. This evidence suggests a potential antagonistic interaction that could compromise the efficacy of this combination therapy.

This presents a paradox, as the impressive clinical outcomes observed with blinatumomab-TKI combinations[13–16,21] challenge the simple prediction of antagonism based solely on *in vitro* data[19], which, by their inherent design, often fail to fully recapitulate the complex cytokine milieu critical for sustained T-cell function *in vivo*. This apparent discrepancy highlights a critical need to understand the factors that may modulate or overcome TKI-mediated suppression of T-cell function. A key question arises from the fact that Src/BCR-ABL1 TKIs- ponatinib and dasatinib are more potent *in vitro* inhibitors of Ph+ALL cells, with

IC50s in the single-digit nanomolar range—one to two orders of magnitude more potent than nilotinib or imatinib. What if the discrepancy is due to faster killing of CD19+ cancer cells that are required to stimulate T-cells *in vitro*, and not due to inhibition of TCR downstream signaling? This result would not be clearly distinguishable in existing literature. So, we aimed to use a modeling approach to test it.

Within this modeling framework, we fit a model and tested two conflicting hypotheses to determine which mechanism best explains the observed T-cell dynamics: (1) that reduced T-cell activity is primarily due to the rapid killing of target B-cells, thereby eliminating the T-cell stimulatory signal, or, (2) the antagonism arises from direct inhibition of T-cell receptor (TCR)-mediated proliferation, through a direct LCK blockade. Our quantitative analysis resolved this conflict: model simulations demonstrated that the observed T-cell dynamics and the antagonistic effect of Src+BCR-ABL1 TKIs could only be accurately recapitulated when the T-cell proliferation rate (parameter p_T) was effectively zeroed out. This result strongly supports direct inhibition of TCR-mediated T-cell proliferation as the dominant factor for the observed antagonism, as simply depleting target cells would not fully explain the T-cell kinetics.

These results led us to investigate whether cytokines could rescue T-cell function by boosting TCR survival signals through a parallel survival pathway. Our findings show that certain interleukins mitigate TKI-induced suppression of blinatumomab activity *in vitro*, enhancing pSTAT5 signaling, which supports T-cell survival and proliferation[22]. These insights potentially explain the favorable clinical outcomes, where such cytokines are naturally present in the body. Moreover, our work provides biological and quantitative evidence to suggest future testing of TKI-BiTE combinations with interleukins in Ph+ ALL.

Methods

Experimental method:

Cell culture and reagents

Experiments were performed using commercially sourced, de-identified PBMCs and established human cell lines. IRB approval was not required. All procedures complied with institutional and national ethical and biosafety guidelines. Jurkat T cells, and BV173 cells were cultured in RPMI 1640 medium supplemented with 10% fetal bovine serum (FBS) and 1% penicillin/streptomycin. Tyrosine kinase inhibitors (TKIs) were used at clinically relevant concentration (CRC) or peak concentrations (Cmax)[19,20]. Blinatumomab was used at 1 ng/mL, and recombinant human IL-2, IL-7, and IL-15 were used at 10 ng/mL.

T-Cell functional assays

T-cell signaling and function were assessed using various assays as previously described[19,20]. LCK phosphorylation was analyzed in Jurkat cells via western blotting and flow cytometry using anti-phospho-LCK (Y394) and total LCK antibodies after TKI pre-treatment and CD3/CD28 stimulation. Luciferase assays were conducted in Jurkat-Luciferase cells co-cultured with BV173 cells and blinatumomab. STAT5

activation was evaluated by western blotting for phospho-STAT5 (Y694) in Jurkat or primary T cells stimulated with interleukins ± TKIs. Combination therapy effects were assessed in primary human T cells co-cultured with BV173 cells, blinatumomab, and/or interleukins, with analysis of CD4, CD8, CD19, and PD-1 expression and viability via flow cytometry. The experimental methods details are fully described in the supplemental experimental methods section.

Modeling method:

To generate data for model development, BV173 B cells and primary T cells were co-cultured at an effector-to-target (E:T) ratio of 1:2 in the presence of blinatumomab (1 ng/mL) for 6 days. Absolute counts of B cells (CD19+), total T cells (CD8+), and exhausted T cells (CD8+PD-1+) were measured daily by flow cytometry.

Two ordinary differential equation (ODE) models were developed to describe co-culture dynamics.

T-B Model: Basic T–B cell interaction: This model includes logistic B cell growth, T cell-mediated B cell killing, T-cell proliferation stimulated by B cells, and natural T-cell death. The ODEs are:

$$\frac{dB}{dt} = r_B\, B\left(1 - \frac{B}{K_B}\right) - a\left(\frac{B^{n_B}}{B^{n_B} + {h_B}^{n_B}}\right)T$$

$$\frac{dT}{dt} = p_T\left(\frac{B^{n_T}}{B^{n_T} + {h_T}^{n_T}}\right)T - d_T\, T$$

Where parameters include (B-cell population), r_B(B-cell growth rate), K_B(B-cell carrying capacity), a(maximum T-cell killing rate), h_B(half-maximal killing constant), n_B(Hill coefficient for killing), T(T-cell population), p_T(T-cell proliferation rate), h_T(half-maximal proliferation constant), n_T(Hill coefficient for proliferation), and d_T(T-cell death rate).

T-B-Tex Model: Incorporating T-Cell exhaustion: T-B-Tex Model extends T-B Model to include exhausted T cells (T_{ex})[23], their generation from active T cells, their suppressive effect on T-cell proliferation, and their own turnover. The expanded ODEs are:

$$\frac{dB}{dt} = r_B\, B\left(1 - \frac{B}{K}\right) - a\left(\frac{B^{n_B}}{B^{n_B} + {h_B}^{n_B}}\right)T$$

$$\frac{dT}{dt} = p_T T\left(\frac{B^{n_T}}{B^{n_T} + {h_T}^{n_T}}\right)\left(\frac{1}{1 + ST_{ex}T_{ex}}\right) - K_{ex}\left(\frac{T^{n_{ex}}}{T^{n_{ex}} + h_{ex}^{n_{ex}}}\right)T - d_T\, T$$

$$\frac{dT_{ex}}{dt} = K_{ex}\left(\frac{T^{n_{ex}}}{T^{n_{ex}} + {h_{T_{ex}}}^{n_{ex}}}\right)T - d_{T_{ex}}\, T_{ex}$$

Additional parameters: (rate of exhaustion), s_{TexT}(T_{ex}-mediated suppressive strength), h_{ex}(half-maximal exhaustion constant), n_{ex}(Hill coefficient for exhaustion), and d_{Tex}(Tex death rate).

Models were fit using a Bayesian framework and Markov Chain Monte Carlo (MCMC) to estimate parameters. Model evaluation metrics and posterior estimates are reported in supplementary Figure 3-4 and Supplementary Tables 1–3. Modeling method is fully described in supplemental modeling method section.

Results

Src/BCR-ABL tyrosine kinase inhibitors antagonize blinatumomab efficacy by suppressing T-cell expansion.

Dasatinib and ponatinib are potent inhibitors of both Src kinases (Src) and the BCR-ABL protein[6,8]. Blinatumomab, a bispecific T-cell engager (BiTE), functions by simultaneously binding to CD3 on T cells and CD19 on malignant B cells, redirecting cytotoxic T lymphocytes to eliminate cancer cells through the formation of an immunological synapse and subsequent perforin/granzyme release. Although clinical combinations of these therapeutics have shown promising results in patients with Philadelphia chromosome-positive acute lymphoblastic leukemia (Ph+ ALL), preclinical studies suggest an antagonistic interaction between TKIs and T-cell function[13,19,21] (Figure 1A).

We evaluated the direct impact of ponatinib on the Ph+ ALL cell line- BV173. Treatment with ponatinib alone resulted in a dose-dependent reduction in BV173 cell viability. Specifically, we observed an approximately 80% reduction in cell viability at concentrations ≥10 nM, consistent with ponatinib's established anti-leukemic activity via BCR-ABL1 inhibition (Figure 1B). We next assessed the efficacy of blinatumomab using a co-culture system of BV173 cells with primary human T cells. Treatment with blinatumomab at concentrations of 0.5 ng/mL and 1 ng/mL induced significant killing of BV173 leukemia cells (Figure 1C). This potent cytotoxicity was accompanied by a robust increase in CD8+ T-cell proliferation (Figure 1C), characteristic of blinatumomab's mechanism of redirecting and activating T cells against CD19+ targets.

We then investigated the combination of blinatumomab (1 ng/mL) with increasing concentrations of ponatinib. This combination effectively reduced BV173 cell viability (Figure 1D). Moreover, T-cell expansion in the presence of blinatumomab combined with ponatinib (at all tested concentrations) was significantly lower (Figure 1D vs Figure 1C, and Figure 1E). The expected combination of ponatinib and blinatumomab effects were calculated using the Bliss independence model. Comparison with the experimentally observed killing revealed a significantly reduced response in the combination group (Bliss score = –18.56), consistent with an antagonistic interaction (Figure 1E).

To determine if this antagonism of T cell function was specific to Src/BCR-ABL1 inhibitors, we compared blinatumomab combinations with SRC-sparing ABL TKIs (imatinib, nilotinib) versus Src/BCR-ABL TKIs

(ponatinib, dasatinib). While all combinations reduced B-cell viability, SFK active ABL inhibitors were less effective, leaving a higher percentage of residual B cells. Crucially, Src/BCR-ABL inhibitors significantly impaired T-cell expansion, which remained near baseline (1–1.5-fold increase). In contrast, imatinib or nilotinib did not impair T-cell proliferation when combined with blinatumomab (Figure 1F). These findings strongly suggest that the Src/BCR-ABL1 TKIs antagonize blinatumomab's T-cell activity, likely due to off-target inhibition of Src kinases like LCK, which are essential for T-cell activation. This is consistent with previous observations[19].

Inhibition of Src/BCR-ABL TKIs inhibits LCK phosphorylation and downstream signaling.

T-cell activation, a complex process essential for adaptive immune responses, is initiated by T-cell receptor (TCR) engagement. Even with stimuli that bypass MHC-antigen presentation, such as CD3/CD28 engagement or BiTE-mediated synapses, the intracellular signaling cascade depends critically on the lymphocyte-specific protein tyrosine kinase LCK.[24] LCK initiates TCR signaling by phosphorylating immunoreceptor tyrosine-based activation motifs (ITAMs) within the CD3 complex, facilitating recruitment and activation of ZAP70.[25] LCK activity is tightly regulated by phosphorylation at tyrosine residue Y394 within its activation loop, which stabilizes its active conformation and is essential for robust downstream signaling[18,26] (Figure 2A).

To test the above pathway and the concordance with prior studies[19], we began by examining their impact on LCK phosphorylation, a critical early event in T-cell receptor (TCR) signaling. Serum-starved Jurkat T-cells were pre-treated with various TKIs at both their clinically relevant (CRC) and peak concentrations (Cmax) for 2-4 hours and then stimulated with CD3/CD28-conjugated dynabeads to activate the TCR pathway. Western blot analysis of LCK phosphorylation at the key tyrosine residue Y394 revealed a significant reduction in phosphorylated LCK (pLCK Y394) in cells treated with ponatinib and dasatinib at both CRC and Cmax (Figure 2B). This inhibitory effect was rapid, becoming evident as early as 30 minutes post-stimulation, with the reduction in pLCK Y394 band intensity consistent with the known inhibitory activity of these drugs against Src kinases, including LCK (FigureS2 A-B). In contrast, cells treated with the BCR-ABL1-selective TKIs imatinib and nilotinib showed no significant change in LCK Y394 phosphorylation compared to stimulated controls (Figure 2B, Figure S2B). These observations were further confirmed and quantified using flow cytometry to analyze intracellular pLCK (Y394) levels in Jurkat T-cells stimulated for 30 minutes and 2 hours. Consistent with our western blot results, treatment with ponatinib or dasatinib resulted in a marked and sustained reduction in the mean fluorescence intensity (MFI) of pLCK (Y394) when measured by intracellular flow cytometry on fixed and permeabilized cells (Figure S2B). Specifically, at 30 minutes, pLCK MFI was reduced by approximately 90% for both ponatinib and dasatinib compared to stimulated control. This significant reduction persisted at 2 hours, with MFI levels remaining approximately 90% lower for both drugs. As observed with western blotting, the selective inhibitors imatinib and nilotinib had no significant effect on LCK phosphorylation under the same condition. These findings provide

compelling evidence that ponatinib and dasatinib potently inhibit LCK phosphorylation, while imatinib and nilotinib do not, reflecting their distinct kinase selectivity profiles.

Following this, we assessed the impact of these TKIs on T-cell proliferation in a more pharmacologically relevant context. We measured the proliferation of total CD3+ T cells and quantified the absolute counts of specific subsets (CD4+ and CD8+) in co-cultures of BV173 leukemia cells and primary human peripheral blood mononuclear cells (PBMCs) after 3 days of treatment. The treatment with Src/BCR-ABL1 TKIs (dasatinib, ponatinib) significantly inhibited the overall expansion of both the CD4+ and CD8+ T-cell populations in the presence of blinatumomab when compared to blinatumomab alone. In contrast, the BCR-ABL1-selective TKIs (imatinib, nilotinib) did not show this inhibitory effect on CD4+ and CD8+ T-cell expansion, further supporting the role of Src kinase inhibition in the observed antagonism (Figure 2C).

To investigate the functional consequences of LCK inhibition on downstream T-cell effector functions, we measured IL-2 production using Jurkat-Luciferase reporter cells. These cells, co-cultured with BV173 leukemia cells and treated with blinatumomab in the presence or absence of TKIs, report IL-2 promoter activity. We found that the Src/BCR-ABL1 TKIs, ponatinib and dasatinib, significantly inhibited blinatumomab-induced IL-2 production. Ponatinib reduced IL-2 production by approximately 30% at its CRC and 80% at its Cmax, while dasatinib reduced it by approximately 50% and 90%, respectively. This demonstrates that the TKI-mediated blockade of LCK phosphorylation directly impairs downstream effector cytokine production (Figure 2D-IL2 activity). To further evaluate the impact on proximal signaling, we measured NFAT-driven luciferase activity, as NFAT is a critical transcription factor in the TCR signaling cascade that regulates IL-2 and other key activation genes. Consistent with the LCK phosphorylation and IL-2 data, ponatinib and dasatinib significantly inhibited NFAT activation at both CRC and Cmax concentrations. Ponatinib reduced NFAT activity by approximately 30% at its CRC and 50% at its Cmax ($p<0.001$), while dasatinib reduced it by approximately 20% and 50% at these concentrations ($p<0.001$). These results collectively demonstrate that Src/BCR-ABL1 TKIs, such as ponatinib and dasatinib, directly inhibit T-cell activation by suppressing phosphorylation of LCK at Y394 (Figure 2D-NFAT activity). This inhibition effectively abrogates proximal TCR signaling, resulting in impaired NFAT activation, diminished IL-2 production, and ultimately, the functional antagonism of blinatumomab-induced T-cell responses. All of this signaling data was consistent with prior observations[19] and is highly suggestive that SFK inhibition downstream of the TCR is the mechanism of ponatinib/dasatinib mediated antagonism of T-cell function. However, the assessment of signaling reductions doesn't precisely specify the mechanism underlying the co-culture effect here. This is because there are two mechanistic paths to reducing TCR signaling in the co-culture experiment.

Mathematical modeling to discern target depletion from direct T-cell inhibition.

The clinical success of combining potent Src/BCR-ABL TKIs (like dasatinib and ponatinib) with blinatumomab presents a paradox when compared to established *in vitro* data, which suggested these agents

antagonize T-cell function by inhibiting the proximal TCR kinase, LCK. This conflict is complicated by a key difference between the TKIs: dasatinib and ponatinib are significantly more potent against BCR-ABL cells than imatinib or nilotinib, raising an ambiguity in the interpretation of the co-culture results. To definitively resolve the mechanism responsible for the observed T-cell suppression *in vitro*, we formally specified two competing hypotheses, as both are possible consequences of using highly potent Src/BCR-ABL TKIs in the co-culture system:

Hypothesis 1: Rapid Target Cell Depletion. Mechanism: Ponatinib and dasatinib are more potent ABL inhibitors than imatinib and nilotinib. This hypothesis posits that the rapid, TKI-mediated elimination of BCR-ABL-dependent B cells removes the necessary antigenic stimulus for sustained TCR activation, leading to reduced T-cell activity. Clinical Significance: If true, the difference between *in vitro* antagonism and clinical success might be attributed to the persistence of physical "safe harbor" sites *in vivo* where Ph+ ALL cells remain during ponatinib treatment, thereby continuously maintaining T-cell stimulation. In this case, combination with blinatumomab may be critical for clearing these residual disease sites (Figure 3A).

Hypothesis 2: Direct Inhibition of T-Cell Activation via LCK/FYN. Mechanism: This proposes the existing hypothesis that Src-family kinase (SFK) inhibition by dasatinib and ponatinib directly impairs TCR-mediated T-cell proliferation and activation through the critical kinases LCK/FYN. This effect is predicted to occur independent of B-cell availability. Clinical Significance: If true, the clinical efficacy suggests that *in vivo* microenvironmental factors—such as naturally occurring cytokines—can overcome or complement the LCK/FYN blockade by engaging a parallel survival or proliferation pathway (Figure 3B).

To evaluate these hypotheses, we reasoned that the quantitative, time-dependent dynamics of the co-culture system would contain sufficient information to unambiguously distinguish between the two mechanisms. We characterized the quantitative dynamics of CD19+ B cells, CD8+ effector T cells, and PD-1+ exhausted T cells in our *in vitro* co-culture system (Figure S3A).

We began by constructing a foundational ordinary differential equation (ODE) model (T-B Model) that described B-cell logistic growth, T-cell-mediated killing, T-cell proliferation, and death (Figure S3B)[18,27]. Parameters were estimated by fitting T-B Model to the experimental data using Markov Chain Monte Carlo[28] (Table S2). While this T-B Model successfully reproduced early B-cell depletion and T-cell expansion, it failed to capture T-cell contraction from day 3 onward. An analysis of the residuals (Figure S3C-D revealed systematic deviations during later stages, indicating a clear model misspecification.

Based on experimental evidence of T-cell exhaustion, we extended the model to the T-B-Tex (Table S3) to explicitly include an exhausted T-cell population alongside functional T cells and B cells[23]. T-B-Tex incorporated transitions from functional T cells to an exhausted state, suppression of functional T-cell proliferation by exhausted T cells, and exhausted T-cell death, and is described in the methods. Fitting this final model to the full dataset using MCMC resulted in a markedly improved agreement with the experimental data, accurately reproducing both the early expansion and subsequent contraction of T cells

(Figure 3C). Residual analysis further confirmed T-B-Tex's superior fit, showing errors that were more randomly distributed around zero with reduced systematic patterns (Figure S4A-B). Model comparison metrics also supported T-B-Tex model: AIC and BIC values were lower despite its greater complexity, and log-likelihood, RMSE, and bias were all improved (Table S1).

The validated T-B-Tex model enabled a direct, *in silico* test of the two hypotheses and a comparison to measured T cell dynamics. Testing Hypothesis 1 (Target Cell Loss): When antagonism was simulated solely by the loss of B-cell stimulation—representing rapid target cell depletion—this mechanism could not reproduce the observed T-cell kinetics (Figure 3A).Testing Hypothesis 2 (Direct T-Cell intrinsic inhibition of LCK/FYN): In contrast, when T-cell proliferation was suppressed *in silico*, Model 2, we observed a flat T cell count at all timepoints (Figure 3B). This was closely recapitulated by the observed T-cell dynamics during combination therapy with Src/BCR-ABL TKIs (Figure 3D). Given the T-cell count data in Figure 3D, we computed the Poisson log-likelihood for both hypotheses under the Blinatumomab + Ponatinib condition. Hypothesis 1 produced a log-likelihood of LL = –7407.142, whereas Hypothesis 2 (B-cell killing plus T-cell inhibition) yielded a dramatically higher log-likelihood of LL = –185.142. This more than 40-fold improvement in likelihood strongly supports Hypothesis 2 as the correct explanation for the observed T-cell dynamics (Table S4).

Collectively, these results resolve the mechanistic uncertainty and demonstrate that the observed antagonistic effect of Src/BCR-ABL TKIs arises primarily from direct inhibition of proximal TCR signaling through LCK and FYN in the T cell, rather than target cell depletion. This also suggests that the origins of the dramatic *in vivo* activity may be through rescuing lost survival signaling through a parallel survival pathway.

Cytokines IL-2, IL-7, and IL-15 rescue the antagonistic effects of Src/BCR-ABL1 TKIs on blinatumomab efficacy.

Based on the concordance between our *in silico* investigation and measured *in vitro* data, which indicated that the antagonistic effect of Src/BCR-ABL1 TKIs on T-cell function is primarily due to LCK/FYN inhibition rather than target cell depletion, we explored biological factors that could resolve the apparent discrepancy between preclinical antagonism and promising clinical outcomes. This led us to test whether cell-intrinsic pathways might rescue T-cell activity.

We evaluated the impact of three common gamma-chain (γc) cytokines—IL-2, IL-7, and IL-15—on blinatumomab-TKI combinations. These interleukins are known regulators of T-cell biology, acting through the JAK-STAT pathway and leading to STAT5 phosphorylation (Figure 4A)[29,30]. IL-2 supports T-cell proliferation and differentiation [31,32] , IL-7 promotes homeostasis and survival [33,34], and IL-15 enhances memory CD8+ T-cell function and expansion[35]. We hypothesized that these cytokines might activate compensatory signaling pathways to bypass the impaired LCK-dependent TCR signaling in the presence of Src/BCR-ABL1 TKIs.

To assess STAT5 activation, Jurkat T-cells were stimulated with 10 ng/mL IL-2, IL-7, or IL-15 (alone or in combination) for 2-4 hours. Cells were treated with TKIs (ponatinib, dasatinib, imatinib, nilotinib) at CRC from the methods and then stimulated for 10 minutes with CD3/CD28 dynabeads. Western blotting for phosphorylated STAT5 (pSTAT5) showed robust activation by each interleukin (Figure 4B), suggesting that γc cytokine signaling remains active across ABL TKIs.

We next tested the functional impact of these cytokines on blinatumomab efficacy in the presence of TKIs. BV173 leukemia cells were co-cultured with T cells and treated with blinatumomab (1 ng/mL) plus each TKI at CRC, with or without IL-2, IL-7, or IL-15 for 2 days. Flow cytometry showed enhanced pSTAT5 signaling with cytokine addition—even in the presence of dasatinib—demonstrating the partial rescue of this key pathway (Figure S5A).

Cytokine addition also significantly improved blinatumomab-mediated cytotoxicity, especially with dasatinib or ponatinib (Figure S6). Among the three, IL-7 produced the strongest effect on T-cell proliferation: a ~2-fold increase with blinatumomab + dasatinib + IL-7 versus blinatumomab + dasatinib alone. The triple combination of blinatumomab, dasatinib, and IL-7 restored CD8 T cell numbers and restored some of the antagonized killing in CD19+ BV173 cells (Figure 4C), indicating IL-7 can partially restore some of the anti-leukemic T-cell activity suppressed by Src/BCR-ABL TKIs *in vitro*.

To further validate the rescue effect, we performed Jurkat-luciferase reporter assays for IL-2 and NFAT. Jurkat cells co-cultured with BV173 cells were treated with blinatumomab (1 ng/mL) and dasatinib (10 nM) for 10 hours, with or without the cytokines. All three cytokines significantly increased IL-2 and NFAT luciferase activity, confirming their ability to restore T-cell activation even under Src kinase inhibition at their CRC concentration (Figure 4D).

We then asked whether these cytokines might also protect against T-cell exhaustion, a key contributor to impaired persistence in bispecific T-cell engager therapies[36] and an effect we observed *in vitro* in Figure 3. Figure 4E shows a schematic of the T-B cell synapse and the PD-1 receptor involved in exhaustion[37,38]. PD-1 expression was quantified after 48 hours in blinatumomab co-cultures (BV173 + T cells, E:T 1:1). Blinatumomab alone induced ~30% PD-1+ T cells. Supplementation with IL-2, IL-7, or IL-15 reduced PD-1 expression, with IL-7 being the most effective at protecting against exhaustion (Figure 4F). This reduction in exhaustion correlates with enhanced cytotoxicity and T-cell proliferation in Figures 4C and S6. It further suggests that mitigating exhaustion is a key mechanism by which γc cytokines—particularly IL-7— might rescue T-cell function in the presence of antagonistic Src/BCR-ABL1 TKIs.

Discussion

The treatment landscape for Ph+ ALL has been transformed by targeted TKIs[8,9,39] and immunotherapies such as blinatumomab[11,40,41]. While combinations of these potent agents hold significant promise[13,15], their optimal integration could be improved through a mechanistic understanding of potential synergistic or antagonistic interactions. Our study provides critical insights into the interaction between Src/BCR-ABL1

TKIs (dasatinib and ponatinib) and blinatumomab-mediated T-cell function, with direct implications for the design of new combination regimens. We rigorously demonstrate that dasatinib and ponatinib, beyond their potent inhibition of BCR-ABL, robustly suppress LCK phosphorylation at Y394—a pivotal step in proximal TCR signaling[18]. This off-target inhibition impairs T-cell proliferation (consistent with prior reports)[19], cytokine production, NFAT activation, and blinatumomab-driven cytotoxicity against leukemia cells. In contrast, SFK sparing BCR-ABL- TKIs such as imatinib and nilotinib, which exhibit minimal SFK inhibition at therapeutic concentrations and preserve blinatumomab's ability to stimulate T-cell responses. [19,20]A key question is how, despite this *in vitro* antagonism, clinical trials combining blinatumomab with dasatinib or ponatinib have demonstrated strikingly favorable outcomes[15].

One remaining question that we addressed in this study is whether the decrease in LCK signaling and antagonism of T-cell activation is upstream or downstream of the TCR. Ponatinib and dasatinib have low single digit nanomolar potency on cells *in vitro*[39,42] while imatinib and nilotinib are significantly less potent. While perhaps less likely, it is formally possible that the kinetics of cell death during a killing assay could deprive the T cell receptor of stimulation—and therefore inducing antagonism and reducing LCK phosphorylation. Measuring LCK phosphorylation in an orthogonal stimulation experiment does not settle this question, but understanding the dynamics of T-cell growth during co-culture with target cells can resolve it unambiguously. To quantitatively dissect this paradox, we employed mathematical modeling to test two competing hypotheses: (1) that antagonism reflects rapid elimination of target B cells, depriving T cells of stimulatory signals, or (2) that it results from direct inhibition of TCR-mediated T cell proliferation through direct inhibition LCK/FYN, independent of target availability. Our model simulations demonstrated that only the suppression of T-cell proliferation in a cell intrinsic manner could recapitulate the observed dynamics, directly supporting the idea that the direct inhibition of TCR signaling through direct inhibition of LCK/FYN—rather than target CD19 cell depletion—is the dominant mechanism of antagonism. While consistent with prior arguments, this dynamics argument adds to our understanding. Disambiguating the mechanism has important implications. By showing that the mechanism is unambiguously downstream of TCR, we raise the possibility that other intracellular signals could compensate for part, or all, of the effect.

A major contribution of this work is identifying IL-7 as a potent mitigator of *in vitro* antagonism. IL-7 restored blinatumomab efficacy and T-cell proliferation in the presence of Src/BCR-ABL1 TKIs, associated with STAT5 activation and reduced T-cell exhaustion. Thus, the clinical success of TKI-Blinatumomab combinations is likely explained by the *in vivo* microenvironment. Blinatumomab infusion is known to induce a transient surge of pro-inflammatory cytokines such as IL2[43], while separate clinical trials of IL-7-secreting ("armored") CAR-T cells have provided clinical proof-of-principle that IL-7 enhances T-cell efficacy in patients[44]. This aligns with our finding that IL-7 can mitigate the antagonism of Src/BCR-ABL1 TKIs on T-cell signaling. These findings suggest that the cytokine-rich *in vivo* microenvironment may help explain the discrepancy between *in vitro* suppression and clinical success. In conclusion, Src/BCR-ABL1 TKIs antagonize blinatumomab by inhibiting LCK-dependent TCR signaling, impairing T-cell activity. IL-7

rescues this effect by restoring proliferation and reducing exhaustion. These results clarify a mechanistic paradox and potentially support cytokine supplementation, particularly IL-7, as a rational strategy to optimize TKI-BiTE combinations in Ph+ ALL.

We acknowledge the limitations of our study, which utilized a simplified *in vitro* system with cell lines and healthy donor PBMCs. This approach was necessary for mechanistic clarity but does not fully recapitulate the dynamic clinical context, including patient heterogeneity and the supportive bone marrow microenvironment. Future work could further validate these findings in more clinically relevant primary patient samples.

Software

Flow cytometry data were analyzed in FlowJo™ v10. Graphs and statistical analyses were performed in Graphpad Prism. The MCMC algorithm was developed and implemented in MATLAB, and all schematic figures were prepared in BioRender.

References:

1. Faderl S, Kantarjian HM, Thomas DA, et al. Outcome of philadelphia chromosome-positive adult acute lymphoblastic leukemia. Leuk Lymphoma. 2000;36(3-4):263-273.
2. Paul S, Kantarjian H, Jabbour EJ. Adult Acute Lymphoblastic Leukemia. Mayo Clin Proc. 2016;91(11):1645-1666.
3. Gleißner B, Gökbuget N, Bartram CR, et al. Leading prognostic relevance of the BCR-ABL translocation in adult acute B-lineage lymphoblastic leukemia: A prospective study of the German Multicenter Trial Group and confirmed polymerase chain reaction analysis. Blood. 2002;99(5):1536-1543.
4. Kantarjian H, Aldoss I, Jabbour E. Management of Adult Acute Lymphoblastic Leukemia: A Review. JAMA Oncol. 2025;11(7):771-778.
5. Soverini S, Hochhaus A, Nicolini FE, et al. BCR-ABL kinase domain mutation analysis in chronic myeloid leukemia patients treated with tyrosine kinase inhibitors: Recommendations from an expert panel on behalf of European LeukemiaNet. Blood. 2011;118(5):1208-1215.
6. Cortes JE, Saglio G, Kantarjian HM, et al. Final 5-year study results of DASISION: The dasatinib versus imatinib study in treatment-Naïve chronic myeloid leukemia patients trial. J Clin Oncol. 2016;34(20):2333-2340.
7. O'Hare T, Deininger MWN, Eide CA, Clackson T, Druker BJ. Targeting the BCR-ABL signaling pathway in therapy-resistant Philadelphia chromosome-positive leukemia. Clin Cancer Res. 2011;17(2):212-221.
8. Aldoss I, Ribera J-M, Kantarjian H, et al. Ponatinib Versus Imatinib in Patients with Newly Diagnosed Ph+ ALL: Subgroup Analysis of the Phase 3 Phallcon Study. Blood. 2023;142(Supplement 1):2871-2871.
9. Jabbour E, Kantarjian H, Aldoss I, et al. S110: Phallcon: a Phase 3 Study Comparing Ponatinib Versus Imatinib in Newly Diagnosed Ph+ All. Hemasphere. 2023;7(S3):e68516d0.
10. Bargou R, Leo E, Zugmaier G, et al. Tumor regression in cancer patients by very low doses of a T cell-engaging antibody. Science. 2008;321(5891):974-977.
11. Kantarjian H, Stein A, Gökbuget N, et al. Blinatumomab versus Chemotherapy for Advanced Acute Lymphoblastic Leukemia. N Engl J Med. 2017;376(9):836-847.
12. Sas V, Moisoiu V, Teodorescu P, et al. Approach to the adult acute lymphoblastic leukemia patient. J Clin Med. 2019;8(8):1182.
13. Foà R, Bassan R, Vitale A, et al. Dasatinib–Blinatumomab for Ph-Positive Acute Lymphoblastic Leukemia in Adults. N Engl J Med. 2020;383(17):1613-1623.
14. Foà R, Bassan R, Elia L, et al. Long-Term Results of the Dasatinib-Blinatumomab Protocol for Adult Philadelphia-Positive ALL. J Clin Oncol. 2024;42(8):881-885.
15. Jabbour E, Short NJ, Jain N, et al. Ponatinib and blinatumomab for Philadelphia chromosome-positive acute lymphoblastic leukaemia: a US, single-centre, single-arm, phase 2 trial. Lancet Haematol. 2023;10(1):e24-e34.

16. Assi R, Kantarjian H, Short NJ, et al. Safety and Efficacy of Blinatumomab in Combination With a Tyrosine Kinase Inhibitor for the Treatment of Relapsed Philadelphia Chromosome-positive Leukemia. Clin Lymphoma Myeloma Leuk. 2017;17(12):897-901.

17. O'Hare T, Walters DK, Stoffregen EP, et al. In vitro activity of Bcr-Abl inhibitors AMN107 and BMS-354825 against clinically relevant imatinib-resistant Abl kinase domain mutants. Cancer Res. 2005;65(11):4500-4505.

18. Palacios EH, Weiss A. Function of the Src-family kinases, Lck and Fyn, in T-cell development and activation. Oncogene. 2004;23(48):7990-8000.

19. Leonard JT, Kosaka Y, Malla P, et al. Concomitant use of a dual Src/ABL kinase inhibitor eliminates the in vitro efficacy of blinatumomab against Ph+ ALL. Blood. 2021;137(7):939-944.

20. Kauer J, Märklin M, Pflügler M, et al. BCR::ABL1 tyrosine kinase inhibitors hamper the therapeutic efficacy of blinatumomab in vitro. J Cancer Res Clin Oncol. 2023;149(2):679-689.

21. Short NJ, Kantarjian HM, Konopleva M, et al. Combination of ponatinib and blinatumomab in Philadelphia chromosome-positive acute lymphoblastic leukemia: Early results from a phase II study. J Clin Oncol. 2021;39(15_suppl):7001.

22. Rochman Y, Spolski R, Leonard WJ. New insights into the regulation of T cells by gamma(c) family cytokines. Nat Rev Immunol. 2009;9(7):480-490.

23. Sahoo P, Yang X, Abler D, et al. Mathematical deconvolution of CAR T-cell proliferation and exhaustion from real-time killing assay data. JR Soc Interface. 2020;17(162):20200747.

24. Courtney AH, Lo WL, Weiss A. TCR Signaling: Mechanisms of Initiation and Propagation. Trends Biochem Sci. 2018;43(2):108-123.

25. Hartl FA, Beck-Garcìa E, Woessner NM, et al. Noncanonical binding of Lck to CD3ε promotes TCR signaling and CAR function. Nat Immunol. 2020;21(8):902-913.

26. Horkova V, Drobek A, Paprckova D, et al. Unique roles of co-receptor-bound LCK in helper and cytotoxic T cells. Nat Immunol. 2023;24(1):174-185.

27. Nägele V, Zugmaier G, Goebeler ME, et al. Relationship of T- and B-cell kinetics to clinical response in patients with relapsed/refractory non-Hodgkin lymphoma treated with blinatumomab. Exp Hematol. 2021;100:32-36.

28. Roy V. Convergence diagnostics for markov chain monte carlo. Annu Rev Stat Appl. 2020;7(1):387-412.

29. Boyman O, Purton JF, Surh CD, Sprent J. Cytokines and T-cell homeostasis. Curr Opin Immunol. 2007;19(3):320-326.

30. Hu X, li J, Fu M, Zhao X, Wang W. The JAK/STAT signaling pathway: from bench to clinic. Signal Transduct Target Ther. 2021;6(1):115.

31. Malek TR. The biology of interleukin-2. Annu Rev Immunol. 2008;26:453-479.

32. Beadling C, Ng J, Babbage JW, Cantrell DA. Interleukin-2 activation of STAT5 requires the convergent action of tyrosine kinases and a serine/threonine kinase pathway distinct from the Raf1/ERK2 MAP kinase pathway. EMBO J. 1996;15(8):1902-1913.

33. Tan JT, Dudl E, LeRoy E, et al. IL-7 is critical for homeostatic proliferation and survival of naïve T cells. Proc Natl Acad Sci U S A. 2001;98(15):8732-8737.

34. Rathmell JC, Farkash EA, Gao W, Thompson CB. IL-7 enhances the survival and maintains the size of naive T cells. J Immunol. 2001;167(12):6869-6876.

35. Waldmann TA. The IL-2/IL-15 receptor systems: targets for immunotherapy. J Clin Immunol. 2002;22(2):51-56.

36. Philipp N, Kazerani M, Nicholls A, et al. T-cell exhaustion induced by continuous bispecific molecule exposure is ameliorated by treatment-free intervals. Blood. 2022;140(10):1104-1118.

37. Chen L, Flies DB. Molecular mechanisms of T cell co-stimulation and co-inhibition. Nat Rev Immunol. 2013;13(4):227-242.

38. Wherry EJ, Kurachi M. Molecular and cellular insights into T cell exhaustion. Nat Rev Immunol. 2015;15(8):486-499.

39. Gozgit JM, Schrock A, Chen T-H, Clackson T, Rivera VM. Comprehensive Analysis Of The In Vitro Potency Of Ponatinib, and All Other Approved BCR-ABL Tyrosine Kinase Inhibitors (TKIs), Against a Panel Of Single and Compound BCR-ABL Mutants. Blood. 2013;122(21):3992.

40. Thomas X. Blinatumomab: a new era of treatment for adult ALL? Lancet Oncol. 2015;16(1):6-7.

41. Topp MS, Gökbuget N, Stein AS, et al. Safety and activity of blinatumomab for adult patients with relapsed or refractory B-precursor acute lymphoblastic leukaemia: a multicentre, single-arm, phase 2 study. Lancet Oncol. 2015;16(1):57-66.

42. Zabriskie MS, Eide CA, Tantravahi SK, et al. BCR-ABL1 Compound Mutations Combining Key Kinase Domain Positions Confer Clinical Resistance to Ponatinib in Ph Chromosome-Positive Leukemia. Cancer Cell. 2014;26(3):428-442.

43. Nägele V, Kratzer A, Zugmaier G, et al. Changes in clinical laboratory parameters and pharmacodynamic markers in response to blinatumomab treatment of patients with relapsed/refractory ALL. Exp Hematol Oncol. 2017;6:14.

44. Lin FY, Stuckert A, Tat C, et al. Phase i Trial of GD2.CART Cells Augmented with Constitutive Interleukin-7 Receptor for Treatment of High-Grade Pediatric CNS Tumors. J Clin Oncol. 2024;42(23):2769-2779.

Figure 1.*Src/BCR-ABL tyrosine kinase inhibitors antagonize blinatumomab efficacy by suppressing T-cell expansion. (A) Schematic illustrating blinatumomab's mechanism of action, in which the CD3–CD19 bispecific T-cell engager links $CD3^+$ T-cells to $CD19^+$ BV173 leukemia cells to promote T-cell–mediated cytotoxicity (B) BV173 leukemia cell viability (Blue-Top) following treatment with increasing concentrations of ponatinib. T-cell proliferation (Red-Bottom) in response to ponatinib alone (C) BV173 cell killing induced by blinatumomab alone (Blue-Top). $CD8^+$ T-cell expansion stimulated by blinatumomab alone (Red-Bottom) (D) BV173 cell numbers in co-cultures treated with combination of blinatumomab (1 ng/mL) and ponatinib (10–40 nM) (Blue-Top). Blinatumomab-induced T-cell proliferation in the presence of ponatinib (Red-Bottom) (E) Comparison of observed versus expected BV173 cell killing under blinatumomab + ponatinib treatment, showing an antagonistic interaction (Bliss score: –18.56). (F) T-cell proliferation in co-cultures treated with blinatumomab and Src/BCR-ABL TKIs (ponatinib, dasatinib) or BCR-ABL–selective TKIs (imatinib, nilotinib). **Statistics:** Data represent mean ± SEM from N = 3 (for panel B-E), N = 6 (for panel F) from primary human T-cell and BV173 co-cultures at an effector:target ratio of 1:2. Statistical significance was assessed using one-way ANOVA with Dunnett's post-hoc test comparing each treatment condition to blinatumomab alone. Significance thresholds: $P<0.05$ (*), $P<0.01$ (**), $P<0.001$(***), $P<0.0001$(****), ns = not significant.

Figure 2:*Inhibition of Src/BCR-ABL TKIs inhibits LCK phosphorylation and downstream signaling. (A) Schematic depicting the role of LCK phosphorylation at Y394 in initiating proximal T-cell receptor signaling and driving downstream activation. (B) Phospho-LCK (Y394) levels in serum-starved Jurkat T cells stimulated with CD3/CD28 in the presence or absence of TKIs. Dual Src/BCR-ABL inhibitors (ponatinib, dasatinib) reduce pLCK Y394, whereas ABL-selective inhibitors (imatinib, nilotinib) show minimal effect. Bar graphs show pLCK normalized to total LCK at Clinically Relevant Concentration (CRC) and Peak concentrations (Cmax). (C) Effects of TKIs on blinatumomab-stimulated T-cell proliferation. $CD8^+$ T-cell proliferation expressed as fold change relative to blinatumomab alone (Left). $CD4^+$ T-cell proliferation expressed as fold change relative to blinatumomab alone (Right). (D) Reporter-based assessment of cytokine and transcriptional activity in the presence of TKIs. IL-2 production quantified using an IL-2 luciferase reporter in Jurkat–BV173 co-cultures treated with blinatumomab (Left). NFAT-dependent luciferase activity measured to evaluate TCR-proximal signaling under TKI treatment (Right). **Statistics:** Data represent mean ± SEM from N = 3 (for panel B, C), N = 5 (for panel D) independent biological replicates. Statistical significance was assessed using one-way ANOVA with Dunnett's post-hoc test comparing each treatment condition to blinatumomab alone. Significance thresholds: $P<0.05$(*), $P<0.01$(**), $P<0.001$(***), $P<0.0001$(****), ns = not significant.

Figure 3.*Mathematical modeling to discern target depletion from direct T-cell inhibition.

A) Hypothesis 1: Model implementation in which rapid B-cell depletion (TKI-mediated B-cell killing rate = 1.1/day) reduces antigen availability and indirectly limits T-cell expansion. (B) Hypothesis 2: Model implementation in which T-cell proliferation is directly inhibited by TKIs ($p_T = 0$), leading to impaired T-

cell expansion and reduced B-cell killing. (C) Schematic and simulation output from the T–B–Tex model showing improved agreement with experimental data, including reproduction of late-phase T-cell decline. The model extends the T–B framework (Fig. S3) by incorporating an exhausted T-cell population (T_{ex}). The schematic depicts transitions among B cells, functional T cells (T), and exhausted T cells (T_{ex}), including the exhaustion rate (k_{ex}) and the suppressive influence of T_{ex} on T-cell activity. (D) Experimental validation of model predictions showing reduced T-cell expansion in combination treatments with Src/BCR-ABL TKIs (ponatinib, dasatinib). Graphs display absolute BV173 cell counts and $CD8^+$ T-cell counts over three days in co-cultures with BV173 cells treated with blinatumomab alone or in combination with Src/BCR-ABL TKIs. **Statistics and Modeling:** Data represent mean ± SEM from N = 6 independent biological replicates. Model fitting and validation were performed using Bayesian parameter estimation with Poisson likelihood and Markov Chain Monte Carlo (MCMC) sampling. Model comparison was based on AIC/BIC criteria.

Figure 4.*Cytokines IL-2, IL-7, and IL-15 rescue the antagonistic effects of Src/BCR-ABL1 TKIs on blinatumomab efficacy.

(A) Schematic illustrating the T-cell activation pathway leading to NFAT and IL-2 production and downstream STAT5 phosphorylation, highlighting the role of LCK Y394 and cytokine receptor signaling (IL-2/IL-7/IL-15). (B) Western blot analysis of pSTAT5 and total STAT5 in Jurkat T cells showing increased STAT5 phosphorylation following addition of IL-2, IL-7, IL-15, and combination of all. (C) T-cell proliferation and BV173 killing in co-cultures treated with dasatinib, with or without IL-2, IL-7, or IL-15. Cytokine addition partially restores $CD8^+$ T-cell proliferation and blinatumomab-mediated BV173 killing in the presence of dasatinib. (D) IL-2 and NFAT luciferase reporter activity in Jurkat cells treated with dasatinib, with or without IL-2, IL-7, or IL-15. Cytokines partially restore IL-2 and NFAT promoter activity after 16 hours. (E) Schematic illustrating T-cell activation and deactivation pathways, including PD-1/PD-L1–mediated inhibitory signaling. (F) Frequency of $PD\text{-}1^+$ $CD8^+$ T cells in co-cultures treated with dasatinib, with or without IL-2, IL-7, or IL-15. **Statistics:** Data represent mean ± SEM from N = 3 (for panel C-F) independent biological replicates Statistical significance was assessed using one-way ANOVA with Dunnett's post-hoc test comparing each condition with the interleukin to no interleukin (control). Significance thresholds: $P<0.05$ (*), $P<0.01$ (*), $P<0.001$ (***), $P<0.0001$(****), ns = not significant.

Figure 1

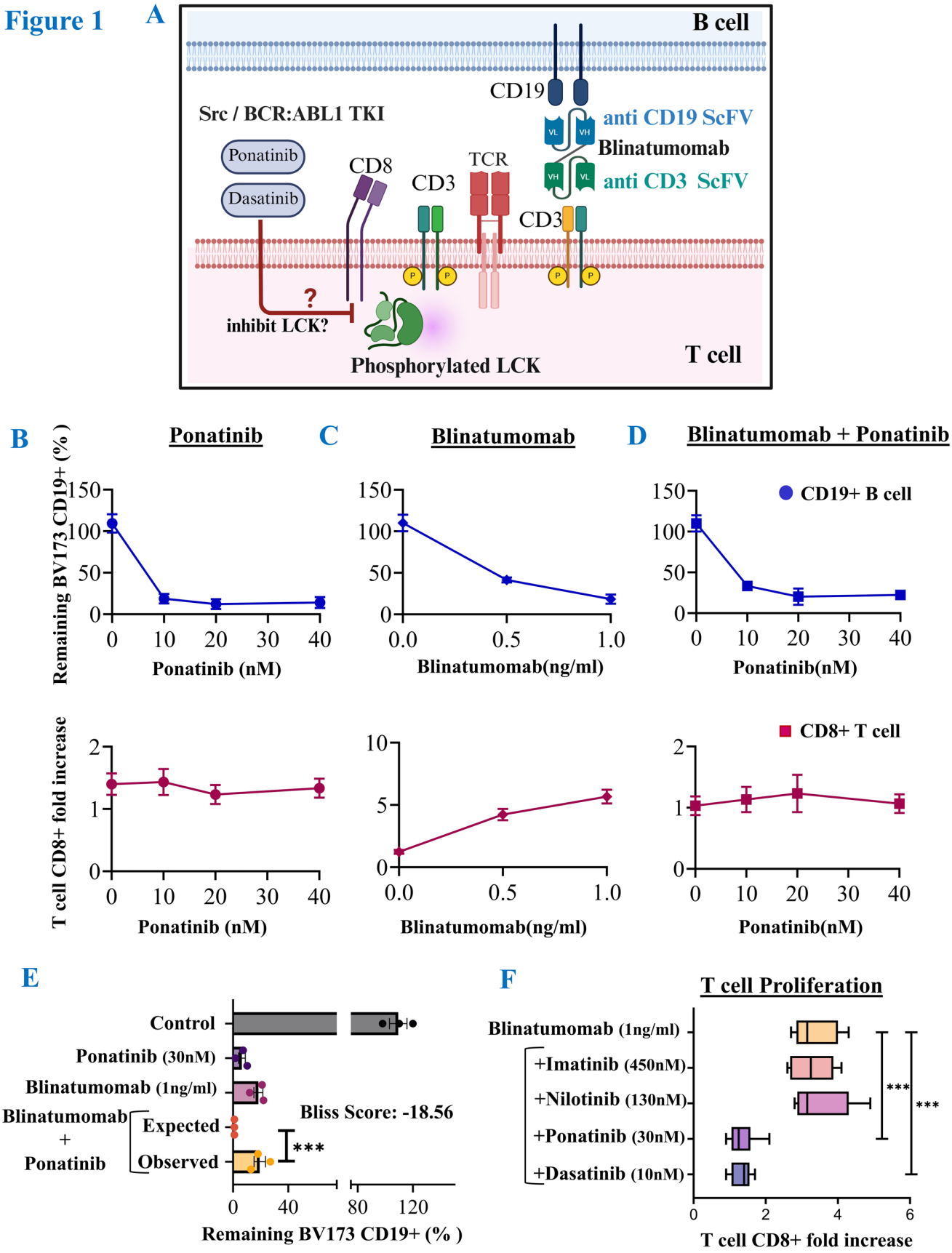
A
B cell
CD19
anti CD19 ScFV
Blinatumomab
anti CD3 ScFV
Src / BCR:ABL1 TKI
Ponatinib
Dasatinib
CD8
CD3
TCR
CD3
?
inhibit LCK?
Phosphorylated LCK
T cell
B
Ponatinib
C
Blinatumomab
D
Blinatumomab + Ponatinib
Remaining BV173 CD19+ (%)
CD19+ B cell
Ponatinib (nM)
Blinatumomab(ng/ml)
Ponatinib(nM)
T cell CD8+ fold increase
CD8+ T cell
Ponatinib (nM)
Blinatumomab(ng/ml)
Ponatinib(nM)
E
Control
Ponatinib (30nM)
Blinatumomab (1ng/ml)
Blinatumomab + Ponatinib
Expected
Observed
Bliss Score: -18.56
***
Remaining BV173 CD19+ (%)
F
T cell Proliferation
Blinatumomab (1ng/ml)
+Imatinib (450nM)
+Nilotinib (130nM)
+Ponatinib (30nM)
+Dasatinib (10nM)
***
***
T cell CD8+ fold increase

Figure 2

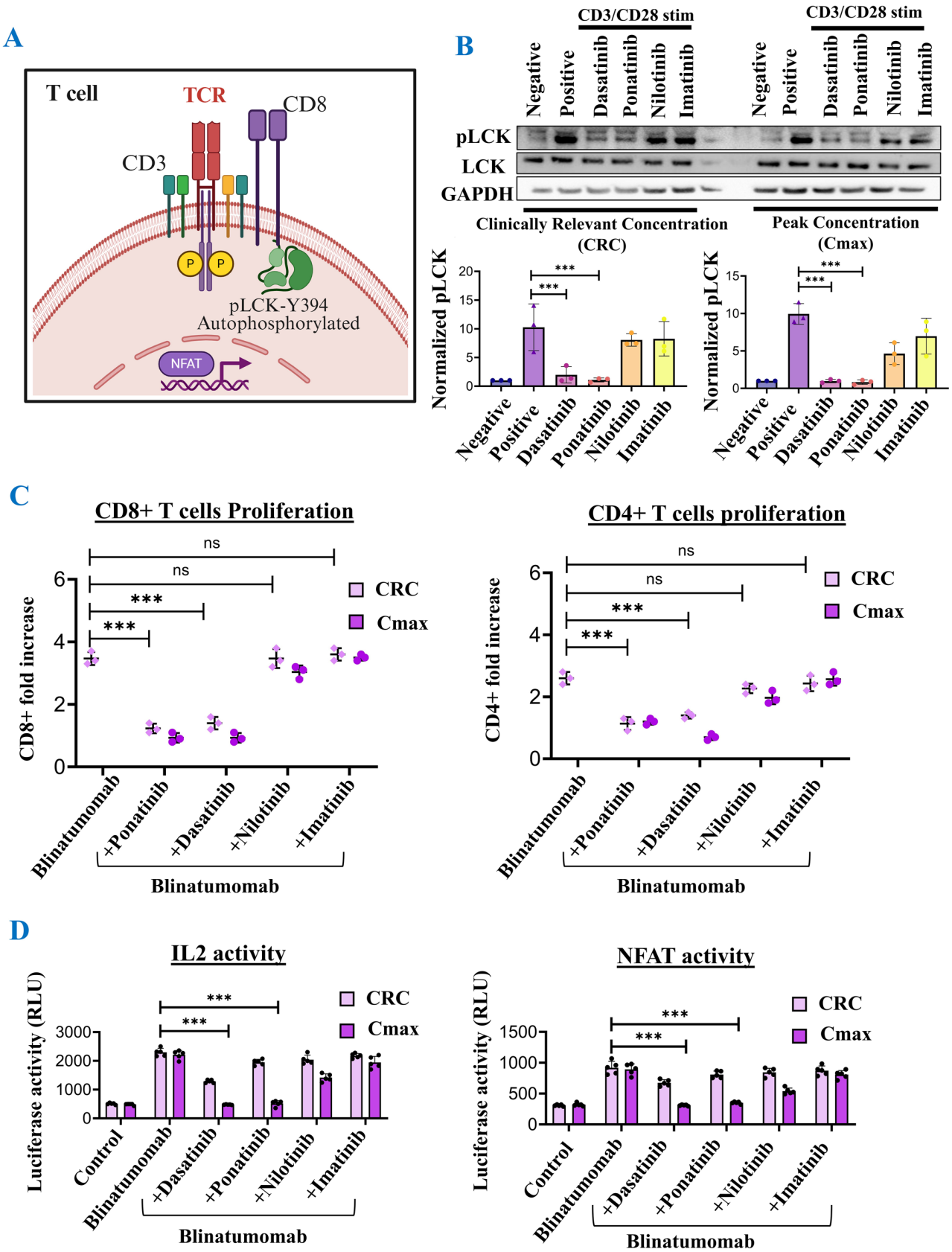
A
T cell
TCR
CD8
CD3
P
P
pLCK-Y394
Autophosphorylated
NFAT
B
CD3/CD28 stim
CD3/CD28 stim
Negative
Positive
Dasatinib
Ponatinib
Nilotinib
Imatinib
pLCK
LCK
GAPDH
Clinically Relevant Concentration (CRC)
Peak Concentration (Cmax)
Normalized pLCK
***
C
CD8+ T cells Proliferation
CD8+ fold increase
ns
CRC
Cmax
Blinatumomab
+Ponatinib
+Dasatinib
+Nilotinib
+Imatinib
Blinatumomab
CD4+ T cells proliferation
CD4+ fold increase
D
IL2 activity
Luciferase activity (RLU)
Control
NFAT activity

Figure 3

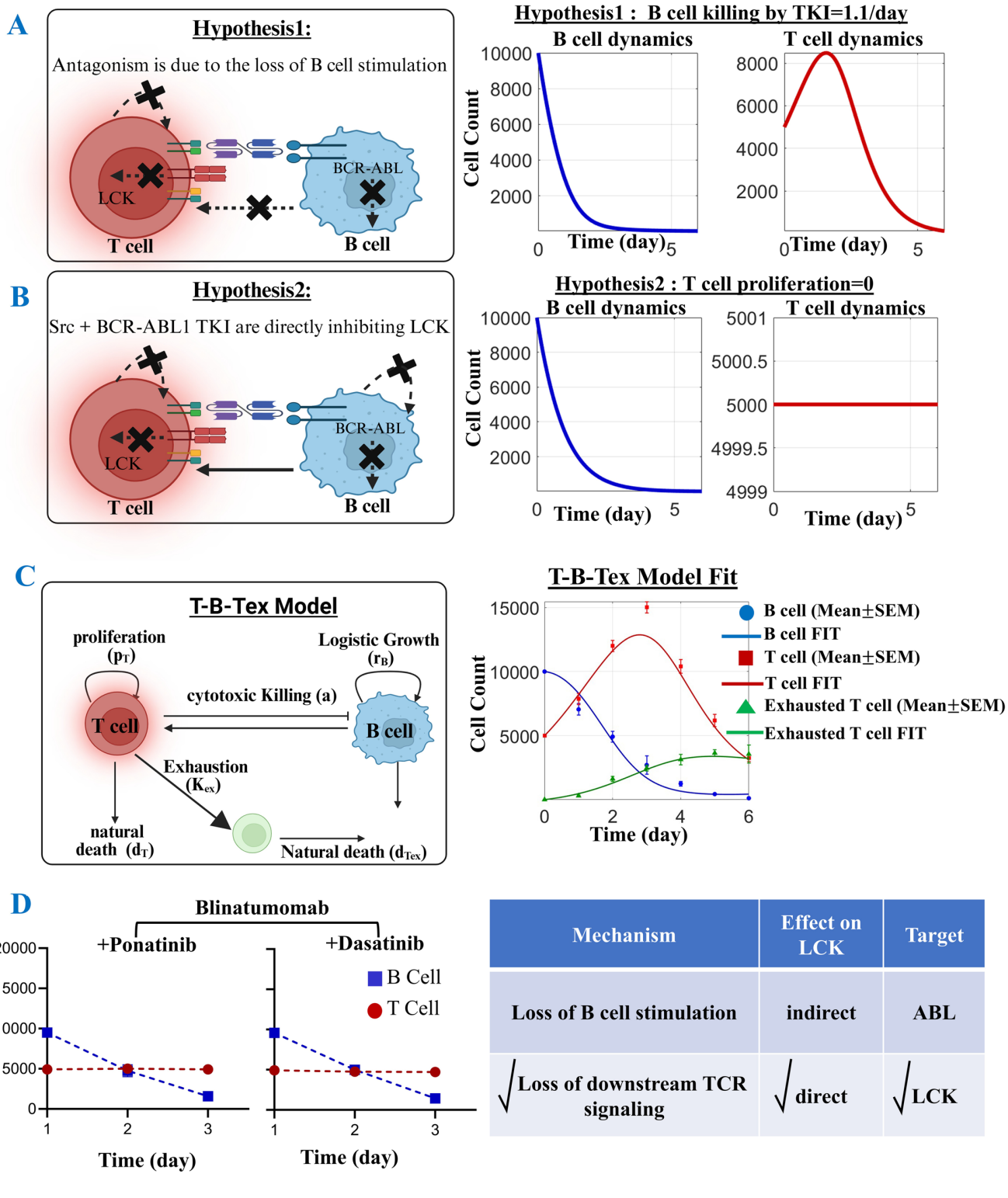

Mechanism	Effect on LCK	Target
Loss of B cell stimulation	indirect	ABL
√ Loss of downstream TCR signaling	√ direct	√ LCK

Figure 4

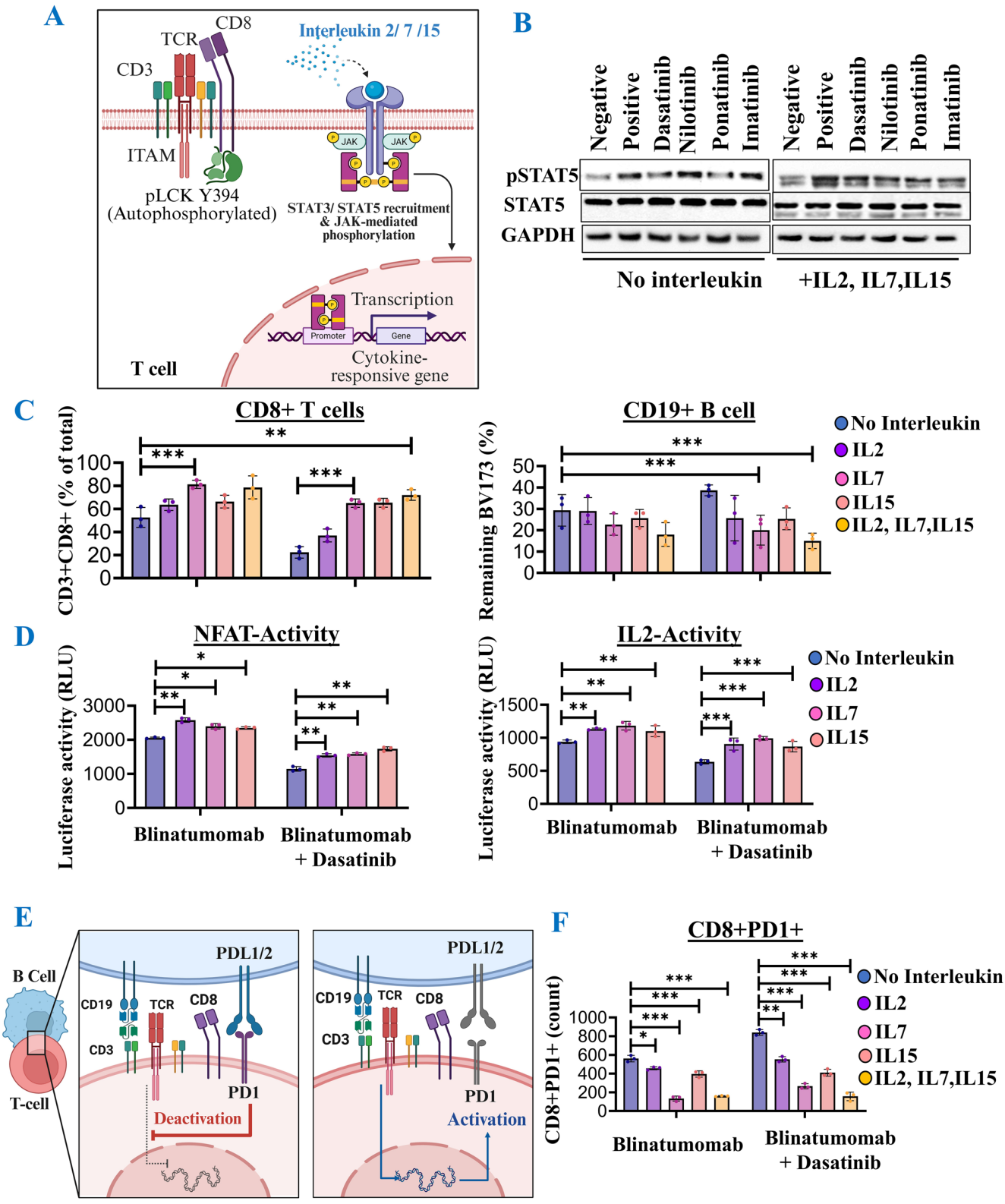
A
CD8
TCR
CD3
ITAM
pLCK Y394
(Autophosphorylated)
Interleukin 2/ 7 /15
JAK
JAK
STAT3/ STAT5 recruitment
& JAK-mediated
phosphorylation
Transcription
Promoter
Gene
Cytokine-
responsive gene
T cell
B
Negative
Positive
Dasatinib
Nilotinib
Ponatinib
Imatinib
Negative
Positive
Dasatinib
Nilotinib
Ponatinib
Imatinib
pSTAT5
STAT5
GAPDH
No interleukin
+IL2, IL7,IL15
C
CD8+ T cells
CD3+CD8+ (% of total)
CD19+ B cell
Remaining BV173 (%)
No Interleukin
IL2
IL7
IL15
IL2, IL7,IL15
D
NFAT-Activity
Luciferase activity (RLU)
IL2-Activity
Luciferase activity (RLU)
Blinatumomab
Blinatumomab
+ Dasatinib
Blinatumomab
Blinatumomab
+ Dasatinib
E
B Cell
T-cell
PDL1/2
CD19
TCR
CD8
CD3
PD1
Deactivation
PDL1/2
CD19
TCR
CD8
CD3
PD1
Activation
F
CD8+PD1+
CD8+PD1+ (count)
No Interleukin
IL2
IL7
IL15
IL2, IL7,IL15
Blinatumomab
Blinatumomab
+ Dasatinib

Supplemental Experimental Methods:

Cell Lines and Primary Cells

The human acute T-cell leukemia cell line Jurkat, Clone E6-1 (ATCC, Cat. No. TIB-152), Jurkat-IL-2-Luciferase, Jurkat-NFAT-Luciferase, and the Philadelphia chromosome-positive (Ph+) pre-B leukemia cell line BV173 (DSMZ, Cat. No. ACC 20) were utilized for this study. All cell lines were maintained in RPMI 1640 Medium (Gibco, Cat. No. 11875093) supplemented with 10% heat-inactivated Fetal Bovine Serum (FBS) (Gibco, Cat. No. 26140079) and 1% Penicillin-Streptomycin (Gibco, Cat. No. 15140122). Cultures were maintained in a humidified incubator at 37°C with 5% CO_2.

Primary human T cells were obtained from peripheral blood mononuclear cells (PBMCs) of two healthy donors purchased from STEMCELL Technologies. T cells were isolated and expanded to >90% purity using the ImmunoCult™ Human CD3/CD28 T Cell Activator kit (STEMCELL Technologies, Cat. No. 10971). For specific T-cell stimulation assays, Dynabeads™ Human T-Activator CD3/CD28 (Thermo Fisher Scientific, Cat. No. 11131D) were used.

Reagents and Therapeutics

Tyrosine Kinase Inhibitors (TKIs): Ponatinib, dasatinib, nilotinib, and imatinib were used. Stock solutions (10–20 mM) were prepared in 100% DMSO and stored at −20°C. Working concentrations were freshly diluted, ensuring the final DMSO concentration in cultures did not exceed 0.1% (v/v).

Clinically relevant concentrations (CRC): ponatinib (30 nM), dasatinib (10 nM), nilotinib (130 nM), imatinib (450 nM)[1];

Peak plasma concentrations (Cmax): ponatinib (145 nM), dasatinib (150 nM), nilotinib (3000 nM), imatinib (3000 nM)[1].

Bispecific T-Cell Engager (BiTE): Blinatumomab (Blincyto®, Amgen) was reconstituted according to supplier instructions and used at a working concentration of 1 ng/mL unless otherwise specified.

Recombinant Interleukins: Recombinant human IL-2 (PeproTech, Cat. No. 200-02), IL-7 (PeproTech, Cat. No. 200-07), and IL-15 (PeproTech, Cat. No. 200-15) were reconstituted per the manufacturer's instructions and stored as aliquots at −20°C. A working concentration of 10 ng/mL was used for all rescue experiments.

T-Cell Stimulation and Signaling Analysis

For LCK phosphorylation analysis, Jurkat T cells were serum-starved overnight. Cells were then pre-treated with TKIs or a vehicle control (0.1% DMSO) for 2-4 hours, followed by stimulation with Dynabeads™ CD3/CD28 or soluble anti-CD3/CD28 antibodies for time points ranging from 10 minutes to 4 hours.

For STAT5 signaling analysis, Jurkat or primary T cells were first stimulated with recombinant interleukins (10 ng/mL) for 4 hours, followed by TKI treatment and a brief 10-minute stimulation with CD3/CD28 Dynabeads before lysis.

Western Blotting

Following stimulation, cells were harvested and lysed on ice using PhosphoSafe™ Extraction Reagent (Millipore Sigma, Cat. No. 71296-3). Total protein concentration was quantified using the Pierce™ BCA Protein Assay Kit (Thermo Fisher, Cat. No. 23225). Equal amounts of protein (10-20 µg) were loaded onto 4-12% NuPAGE™ Bis-Tris precast gels (Invitrogen) and resolved by SDS-PAGE using NuPAGE™ MOPS SDS Running Buffer. Proteins were transferred to a nitrocellulose membrane using NuPAGE™ Transfer Buffer. Membranes were blocked for 1 hour with 5% Bovine Serum Albumin (BSA) in TBST and incubated overnight at 4°C with the following primary antibodies:

anti-phospho-LCK (Y394) (R&D Systems, Cat. No. MAB8138), anti-total LCK (Cell Signaling Technology, Cat. No. 2785), anti-phospho-STAT5 (Y694) (Cell Signaling Technology, Cat. No. 9359), anti-total STAT5 (Cell Signaling Technology, Cat. No. 94205), and anti-GAPDH (Cell Signaling Technology, Cat. No. 5174). Membranes were then incubated with HRP-conjugated secondary antibodies (Cell Signaling Technology), and protein bands were visualized using SuperSignal™ West Pico PLUS Chemiluminescent Substrate (Thermo Fisher, Cat. No. 34580).

Flow Cytometry

For intracellular analysis of LCK phosphorylation, stimulated Jurkat cells were fixed with 4% paraformaldehyde (BioLegend, Cat. No. 420801) and then permeabilized using TruPhosPho™ Perm Buffer (BioLegend, Cat. No. 425801). Cells were subsequently stained with PE anti-human phospho-LCK (Y394) antibody (BioLegend, Cat. No. 651203).

For co-culture assays, cells were harvested and stained with a surface antibody cocktail to identify and quantify distinct cell populations. The panel included the following antibodies, all from BioLegend: FITC anti-human CD4 (Clone RPA-T4, Cat. No. 300506), PE anti-human CD8 (Clone RPA-T8, Cat. No. 301008), APC anti-human CD19 (Clone HIB19, Cat. No. 302212), and PE/Cy7 anti-human PD-1 (Clone EH12.2H7, Cat. No. 329918). Cell viability was assessed using the Zombie NIR™ Fixable Viability Kit (BioLegend, Cat. No. 423105). To determine absolute cell counts, Precision Count Beads™ (BioLegend, Cat. No. 424902) were added to each sample prior to acquisition.

All data were acquired on a BD LSRFortessa™ cell analyzer and were analyzed using FlowJo™ software.

Functional T-Cell Assays

Luciferase Reporter Assays: Jurkat-IL-2-Luciferase or Jurkat-NFAT-Luciferase reporter cells were pre-treated with TKIs for 2-4 hours before being co-cultured with BV173 target cells (E:T ratio 1:1) and blinatumomab (1 ng/mL) for 16 hours. Luciferase activity was measured using the Luciferase Assay System (Promega, Cat. No. E1500) on a multimode plate reader EnVision™. Combination Therapy and Cytotoxicity Assays: Primary human T cells were co-cultured with BV173 target cells (E:T ratio 1:2) for 48-72 hours in the presence of blinatumomab, TKIs, and/or interleukins. For rescue experiments, T cells were pre-incubated overnight with interleukins prior to co-culture. Target cell killing and T-cell proliferation were assessed by flow cytometry.

Supplemental Modeling Methods

Bliss Score

To quantify pharmacologic interaction, we applied the Bliss independence model[2]. Fractional killing for each single agent (Ponatinib and Blinatumomab) was used to calculate the expected additive effect using:

$$E_{A+B} = E_A + E_B - (E_A \cdot E_B)$$

The Bliss score was defined as the difference between the observed combination effect and the predicted Bliss value, with negative values indicating antagonism.

Parameter Estimation and Model Fitting

Parameters for both Model 1 and Model 2 were estimated by fitting the model equations to the experimental time-course data. This was accomplished using a Bayesian framework with Markov Chain Monte Carlo (MCMC) algorithms implemented in MATLAB.

Bayesian Framework and Likelihood Function

The log-likelihood function, which quantifies the probability of observing the experimental data given a specific set of model parameters, was custom-defined assuming a Poisson-distributed measurement error for the cell counts.

Prior Distributions

For each parameter to be estimated, non-informative or weakly informative prior distributions were defined based on existing literature and biological plausibility. This approach constrains the parameter space to reasonable bounds, a critical step in Bayesian inference.

MCMC Methodology:

The log-likelihood function, which quantifies the probability of observing experimental data given a set of parameter values, was custom-defined assuming a Poisson distribution for the measurement error of the cell counts. For each model, 3 independent MCMC chains were initiated. Each chain was run for a total of 10^6 to 10^7 iterations[3,4]. The initial 20-30% of iterations from each chain were discarded as burn-in (based on the parameter that convergence took longer). The post-burn-in chains were thinned by selecting every 100th iteration to reduce autocorrelation, resulting in posterior samples for each parameter.

Convergence Diagnostics:

Trace plots: Visual inspection for mixing and stationarity (Figure S3C-S4A).

Gelman-Rubin statistic ($\hat{R}$): All parameters had $\hat{R} < 1.1$, indicating convergence.

Effective sample size (ESS): All ESS > 1000 (indicative of adequate sampling).

Model Fit Evaluation: The goodness-of-fit of each calibrated model to the experimental data was evaluated both visually and quantitatively. Visual assessment involved overlaying the model simulation (mean of the posterior parameter estimates) against the experimental time-course data (mean ± SEM) (Figure 3A - Figure S3B).

Quantitative metrics used to assess model fit and compare model performance included:

Log-Likelihood (LL): The log-likelihood value calculated at the mean posterior parameter estimates. The log-likelihood quantifies the probability of observing the experimental data given the model and a specific set of parameters. Higher LL values indicate a better fit.

Akaike Information Criterion (AIC): Calculated as $AIC = 2k - 2\ln(LL)$, where k is the number of estimated parameters and LL is the log-likelihood. AIC estimates the relative amount of information lost by a given model and provides a measure of model fit that penalizes for the number of parameters. Lower AIC values indicate a better balance between goodness-of-fit and model complexity.

Bayesian Information Criterion (BIC): Calculated as $BIC = k\ln(n_{obs}) - 2\ln(LL)$, where k is the number of estimated parameters, nobs is the total number of observations used for fitting, and LL is the log-likelihood. Similar to AIC, BIC penalizes for the number of parameters, but applies to a stronger penalty than AIC, particularly for larger datasets. Lower BIC values indicate a preferred model.

For both AIC and BIC, lower values indicate a more parsimonious model that provides a better balance between goodness-of-fit and complexity. The final values for these metrics used for model comparison are provided in Table S1

Table S1: Model Evaluation

Model	k_{free}	n_{obs}	Log Likelihood Mean	AIC	BIC
Model 1	5	84	-9975.1	19960.3	19972.5
Model 2	9	126	-16264.5	2547.08	3257.6

The final parameter estimates for Model 1 (Table S2) and Model 2 (Table S3) were determined by fitting the models to the experimental data.

T-B Model: Basic T–B cell interaction [5–7]**:**

$$\frac{dB}{dt} = r_B\, B\left(1 - \frac{B}{K_B}\right) - a\left(\frac{B^{n_B}}{B^{n_B} + {h_B}^{n_B}}\right)T$$

$$\frac{dT}{dt} = p_T\left(\frac{B^{n_T}}{B^{n_T} + {h_T}^{n_T}}\right)T - d_T\, T$$

Table S2: T-B parameter estimates

T-B Model	Meaning	Units	Priors	Final Estimation
$\mathbf{r_B}$	B cell growth rate	Day^{-1}	fixed	0.63
K	B cell carrying capacity	Cells/ml	fixed	$0.24*10^6$
a	Max killing rate of B cells by T cells	rate × $cells^{-1}$	[0.5,6]	1.6
nB	Hill coefficient for T-mediated killing of B cells	dimensionless	fixed	1
hB	Half-saturation for B cell killing	Cells/ml	[0.01-0.2] $*10^6$	$0.062*10^6$

nT	Hill coefficient for T cell proliferation	dimensionless	fixed	1
h_T	Half-saturation for B-driven T cell proliferation	cells	[0.0001-0.009] *10^6	0.007*10^6
p_T	T cell proliferation rate	Day $^{-1}$	[0.1-3]	1.98
dT	T cell death rate	Day $^{-1}$	[0.001-1.5]	1.2

T-B-Tex Model [8]:

$$\frac{dB}{dt} = r_B\, B\left(1 - \frac{B}{K}\right) - a\left(\frac{B^{n_B}}{B^{n_B} + {h_B}^{n_B}}\right)T$$

$$\frac{dT}{dt} = p_T T\left(\frac{B^{n_T}}{B^{n_T} + {h_T}^{n_T}}\right)\left(\frac{1}{1 + ST_{ex}T_{ex}}\right) - K_{ex}\left(\frac{T^{n_{ex}}}{T^{n_{ex}} + h_{ex}^{n_{ex}}}\right)T - d_T\, T$$

$$\frac{dT_{ex}}{dt} = K_{ex}\left(\frac{T^{n_{ex}}}{T^{n_{ex}} + {h_{T_{ex}}}^{n_{ex}}}\right)T - d_{T_{ex}}T_{ex}$$

Table S3: T-B-Tex parameter estimates

T-B-Tex Model	Meaning	Units	Priors	Final Estimation
r_B	B cell growth rate	Day $^{-1}$	fixed	0.63
K_B	B cell carrying capacity	cells	fixed	0.24*10^6
a	Max killing rate of B cells by T cells	rate × cells^{-1}	[1,8]	3.75
n_B	Hill coefficient for T-mediated killing of B cells	dimensionless	fixed	1
h_B	Half-saturation for B cell killing	Cells/ml	[.005,.04] *10^6	0.032*10^6
n_T	Hill coefficient for T cell proliferation	dimensionless	fixed	1
h_T	Half-saturation for B-driven T cell proliferation	Cells/ml	[.0001-0.015] *10^6	0.001*10^6
p_T	T cell proliferation rate	Day $^{-1}$	[0.5-5]	1.87
d_T	T cell death rate	per day	[0.005-1.5]	0.011
k_{ex}	Exhausted T cell growth rate	Day $^{-1}$	[0.05-5]	0.17

n_{ex}	Hill coefficient for exhausted T cell proliferation	dimensionless	fixed	1
h_{ex}	Half-saturation for T cell driven proliferation	Cells/ml	[0.03-0.25]*10^6	0.006*10^6
dT_{ex}	Death rate of the exhausted T cell	Day $^{-1}$	[0.005-0.1]	0.12
sT_{exT}	suppression strength of Tex on T proliferation	Day $^{-1}$	[1e-7- 0.1]	8.15*10^{-8}

Hypothesis testing:

We tested two alternative TKI mechanisms by simulating the T–B–Tex model under two conditions: (1) H1, where TKIs act only on leukemic B cells by adding a constant 1.1/day B-cell killing term while keeping all T-cell parameters unchanged, and (2) H2, where TKIs both kill B cells and fully inhibit T-cell functions by setting $p_T = 0$, $d_T = 0$, and $K_{ex} = 0$. For each hypothesis, simulated T-cell trajectories were compared to experimental T-cell data using a Poisson log-likelihood, and a likelihood-ratio test determined which hypothesis better explained the observed T-cell behavior. We compared the simulated T-cell trajectories from each hypothesis to the experimental data using a Poisson log-likelihood and selected the model with the higher likelihood (Table S4). In both dasatinib- and ponatinib-treated conditions, H2 consistently achieved a dramatically higher likelihood than H1, leading to the selection of H2 as the mechanism best supported by the data

Table S4: Hypothesis testing using Poisson log-likelihood

Condition	LL(H1)	LL(H2)	Hypothesis Chose
Dasatinib + Blinatumomab	−8627.447	−424.705	H2
Ponatinib + Blinatumomab	−7407.142	−185.142	H2

Model Script:

Model T-B Folder:

i. TB model_fixed: ODE Function for Model T-B
ii. runMCMC_TB_fixed: MCMC function for Model T-B
iii. PriorFunction_fixed: Prior Function for Model T-B
iv. Loglikelihood_TB_fixed: Loglikelihood function for model T-B
v. Model1: main script

Model T-B-Tex Suppression Term Folder:

i. B_T_Tex_Model_v3: ODE Function for Model T-B-Tex
ii. runMCMC_v3: MCMC function for Model T-B-Tex
iii. loglikelihood_v3: Loglikelihood function for Model T-B-Tex
iv. PriorFunction_v3: Prior Function for Model T-B-Tex

v. runMCMC_v3

vi. newcode_Suppressionterm: main script

Hypothesis Testing Folder:

i. Test_drug_hypothesis: Hypothesis 1 and Hypothesis 2 testing

ii. Poisson_loglik: poisson likelihood function for calculating Loglikelihood

References

1. Liu C, Leighow SM, McIlroy K, et al. Excessive concentrations of kinase inhibitors in translational studies impede effective drug repurposing. Cell Rep Med 2023;4(10):101227.

2. Foucquier J, Guedj M. Analysis of drug combinations: current methodological landscape. Pharmacol Res Perspect;3(3):.

3. Roy V. Convergence diagnostics for markov chain monte carlo. Annu Rev Stat Appl 2020;7387–412.

4. Xing LEP. 16 : Approximate Inference : Markov Chain Monte Carlo Markov Chain Monte Carlo Concept of Markov Chain. 2017;1–9.

5. Nägele V, Zugmaier G, Goebeler ME, et al. Relationship of T- and B-cell kinetics to clinical response in patients with relapsed/refractory non-Hodgkin lymphoma treated with blinatumomab. Exp Hematol 2021;10032–36.

6. Dritschel H, Waters SL, Roller A, Byrne HM. A mathematical model of cytotoxic and helper T cell interactions in a tumour microenvironment. Lett Biomath 2018;5(sup1):S36–S68.

7. Hosseini I, Gadkar K, Stefanich E, et al. Mitigating the risk of cytokine release syndrome in a Phase I trial of CD20/CD3 bis pecific antibody mosunetuzumab in NHL: impact of translational system modeling. NPJ Syst Biol Appl;6(1):.

8. Sahoo P, Yang X, Abler D, et al. Mathematical deconvolution of CAR T-cell proliferation and exhaustion from real-time killing assay data. J R Soc Interface;17(162):.

Figure S1

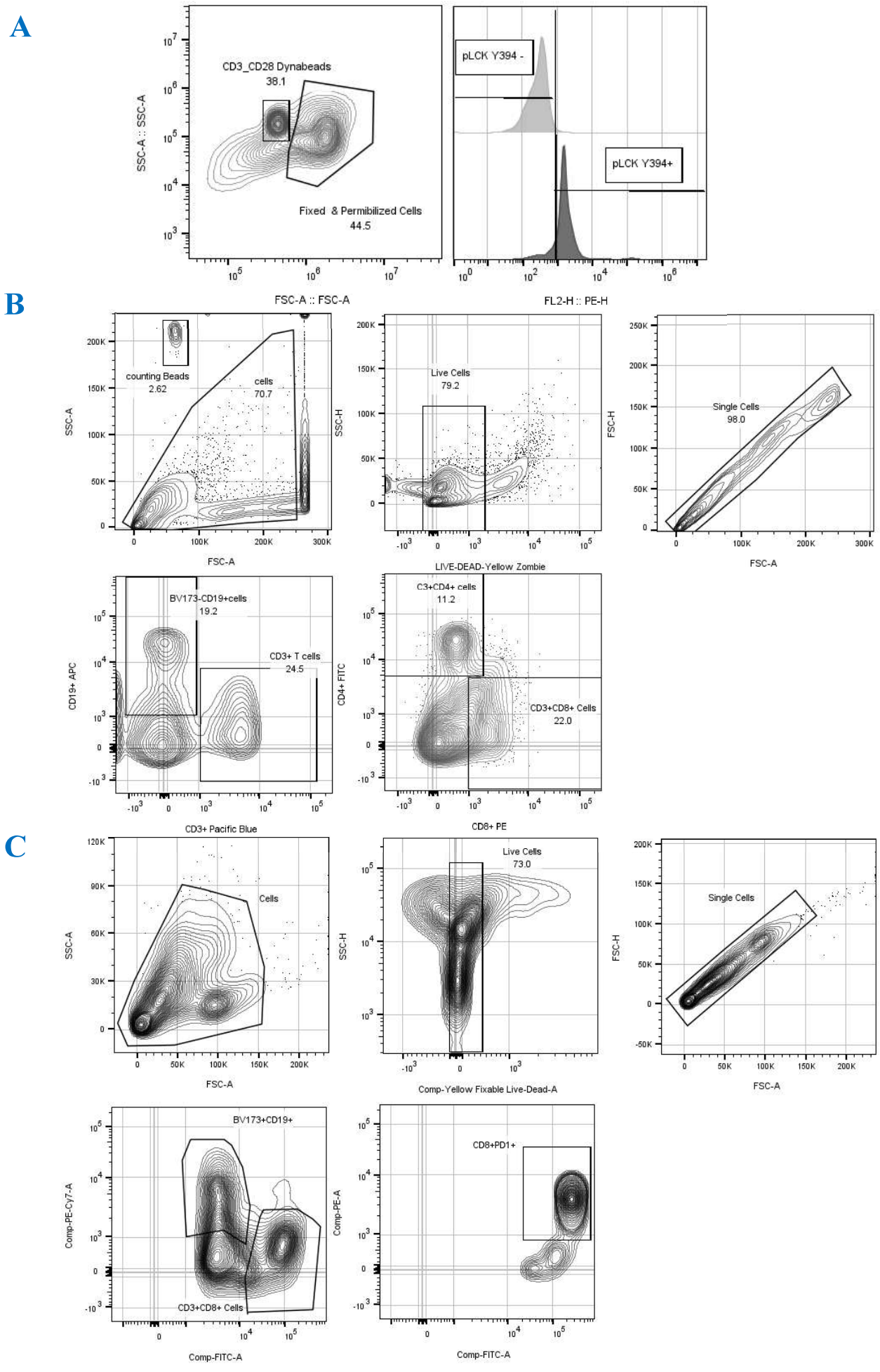
A
CD3_CD28 Dynabeads
38.1
Fixed & Permibilized Cells
44.5
SSC-A :: SSC-A
pLCK Y394 -
pLCK Y394+
B
FSC-A :: FSC-A
counting Beads
2.62
cells
70.7
SSC-A
FSC-A
SSC-H
FL2-H :: PE-H
Live Cells
79.2
FSC-H
Single Cells
98.0
FSC-A
BV173-CD19+cells
19.2
CD3+ T cells
24.5
CD19+ APC
CD3+ Pacific Blue
LIVE-DEAD-Yellow Zombie
C3+CD4+ cells
11.2
CD3+CD8+ Cells
22.0
CD4+ FITC
CD8+ PE
C
Cells
SSC-A
FSC-A
Live Cells
73.0
SSC-H
Comp-Yellow Fixable Live-Dead-A
Single Cells
FSC-H
FSC-A
BV173+CD19+
CD3+CD8+ Cells
Comp-PE-Cy7-A
Comp-FITC-A
CD8+PD1+
Comp-PE-A
Comp-FITC-A

Figure S1.* Gating strategy for Flow Cytometry Analysis. (A) Phospho-LCK analysis in Jurkat cells. Serum-starved cells were treated with TKIs for 2–4 hours, stimulated with CD3/CD28 Dynabeads (1:2), then fixed, permeabilized, and stained with a PE-conjugated antibody specific for pLCK Y394. $pLCK^+$ cells were quantified based on PE signal. (B) Co-culture analysis for combination treatments. Live cells were identified as Zombie Yellow–negative, and singlets were gated using FSC/SSC. Within singlets, T cells were gated as $CD3^+CD8^+$ and BV173 leukemia cells as $CD19^+$. (C) Gating for modeling-related experiments. Live Zombie Yellow–negative singlets were gated using FSC/SSC, followed by staining with CD8 and CD19. $CD8^+$ T cells were gated, and PD-1 expression was assessed within the $CD8^+$ population**.**

Figure S2

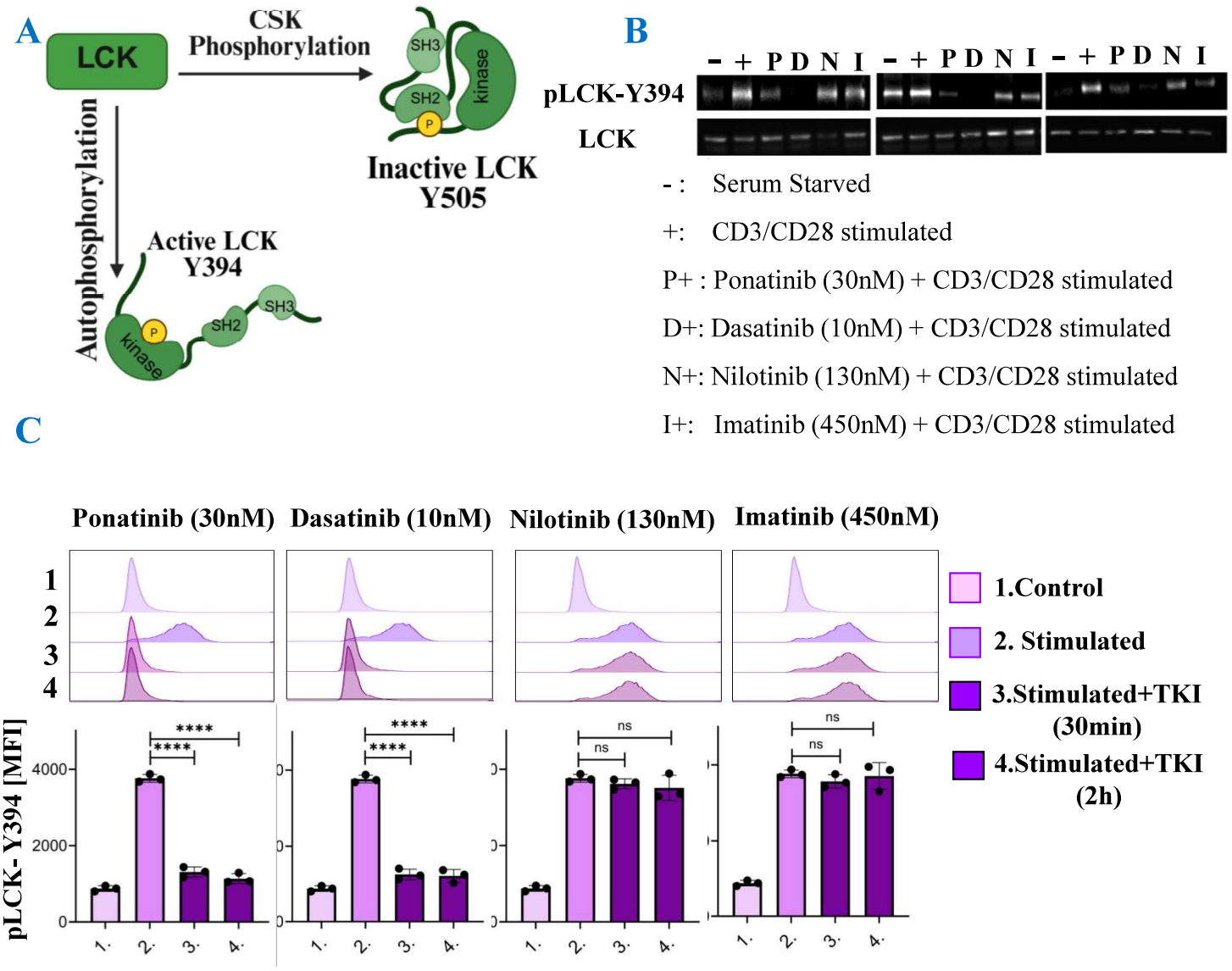

Figure S2. Rapid inhibition of LCK by Src tyrosine kinase inhibitors (TKIs). (A) Schematic illustrating regulation of LCK activity through phosphorylation of Y394 and Y505. Autophosphorylation at Y394 promotes TCR-proximal signaling, whereas CSK-mediated phosphorylation of Y505 inhibits LCK activity. (B) Western blot analysis of pLCK Y394 in serum-starved Jurkat cells treated with Src TKIs—ponatinib (P+), dasatinib (D+), nilotinib (N+), or imatinib (I+)—followed by CD3/CD28 stimulation. LCK Y394 levels were examined for 30 minutes, 2 hours, and 4 hours. (C) Flow-cytometric analysis of intracellular pLCK Y394 in Jurkat cells treated with TKIs at their clinically relevant concentrations for 2 hours and stimulated with CD3/CD28 for 30 minutes or 2 hours. Mean fluorescence intensity (MFI) values are shown for each condition.

Figure S3

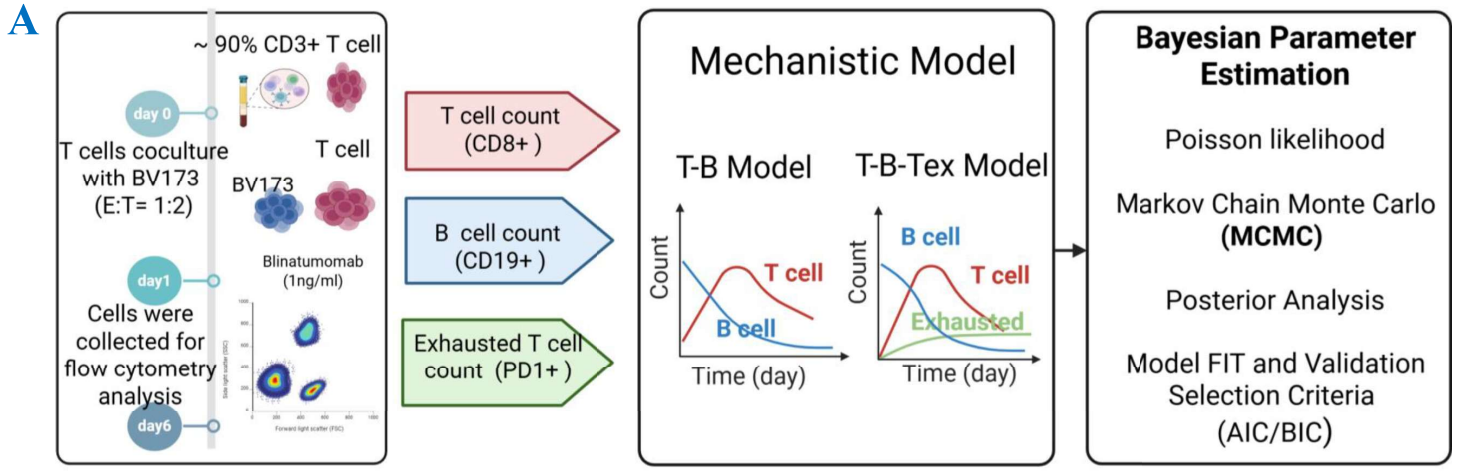

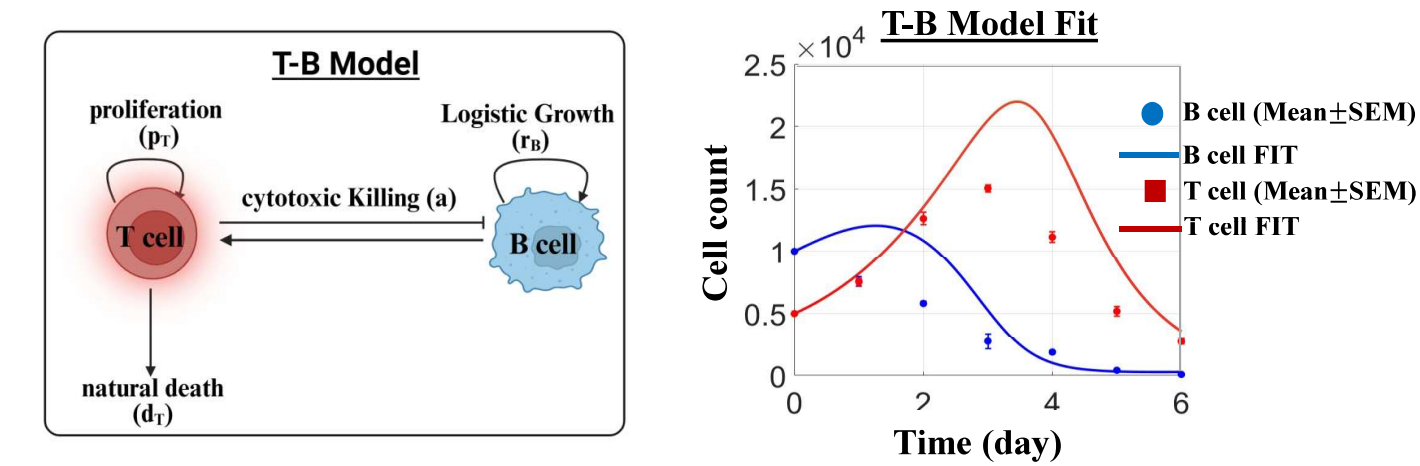

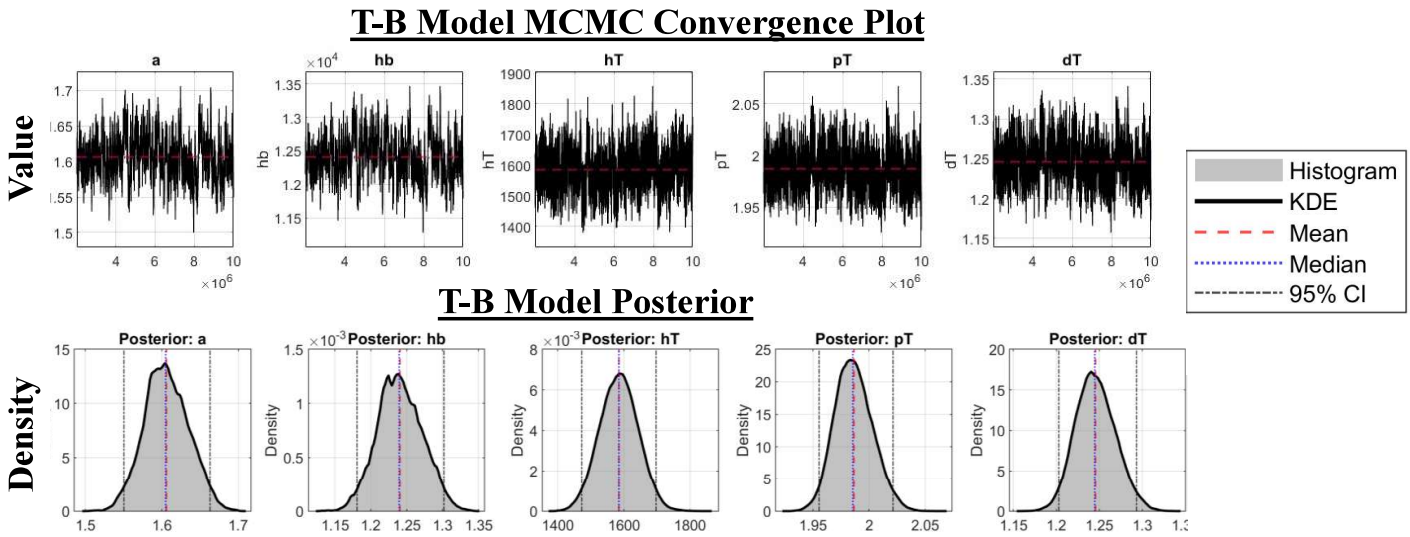

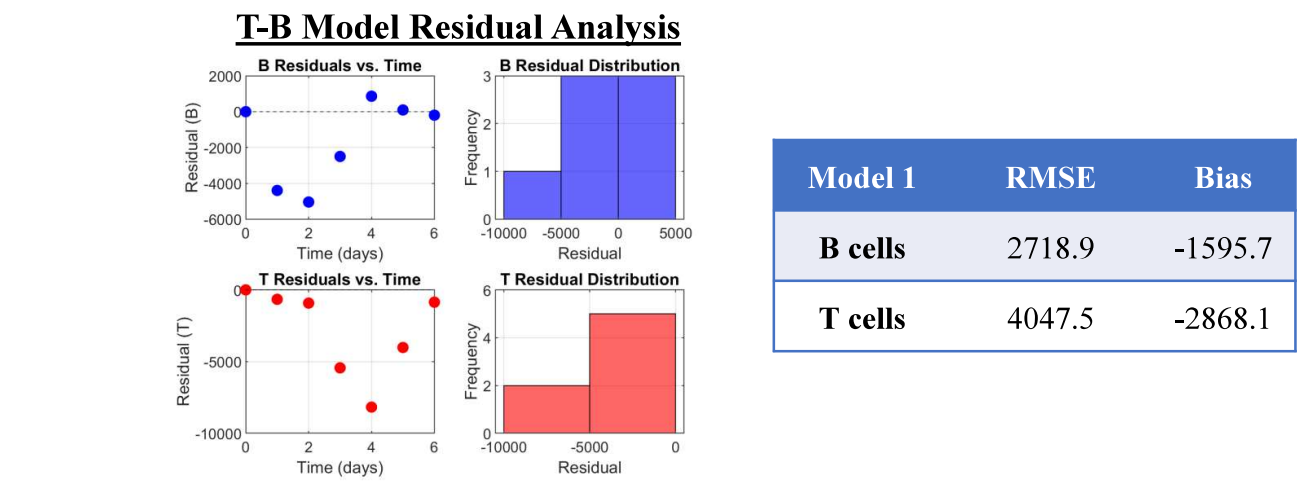

Model 1	RMSE	Bias
B cells	2718.9	-1595.7
T cells	4047.5	-2868.1

Figure S3:*Markov Chain Monte Carlo (MCMC) and residual analysis for model 1 parameter estimation. (A) Experimental setup for quantifying $CD19^+$ B cells, $CD8^+$ T cells, and $PD\text{-}1^+$ exhausted T cells in blinatumomab-treated co-cultures. Primary T cells and BV173 cells were plated at an effector-to-target ratio of 1:2 in round-bottom 96-well plates. Six independent replicates were analyzed daily for six days by flow cytometry. Gating strategy is shown in Supplementary Figure S1C. (B) Overview of the mathematical framework used for Model 1. An ordinary differential equation (ODE) model was constructed to describe temporal changes in B cells and T cells. Parameters were estimated using Markov Chain Monte Carlo (MCMC) fitting to experimental data. Model 1 includes logistic B-cell growth (rB, KB), T-cell-mediated B-cell killing (a, nB, hB), B-cell-dependent T-cell proliferation (pT, nT, hT), and natural T-cell death (dT). (C) MCMC results for Model 1 parameter estimation. Trace plots show mixing and convergence of sampled parameter values. Corresponding posterior distributions indicate parameter ranges and uncertainty. (D) Residual analysis comparing Model 1 predictions with experimental B-cell and T-cell counts over six days. Residuals are shown for all timepoints and both cell populations.

Figure S4

A

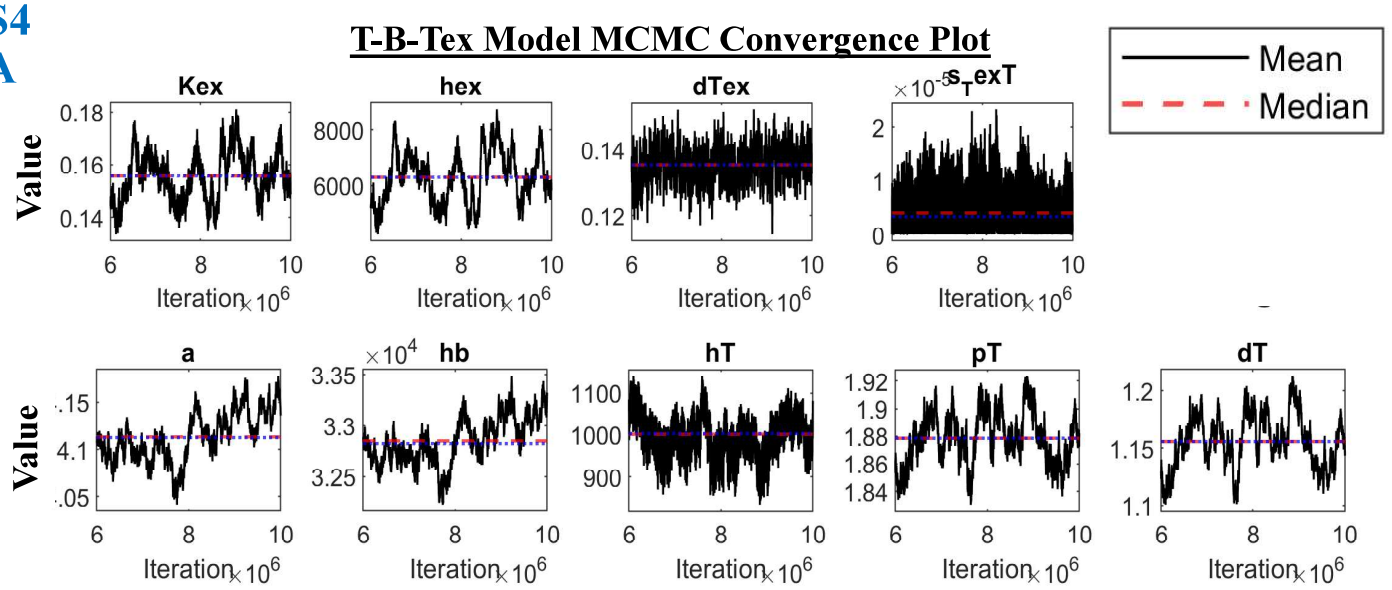

B

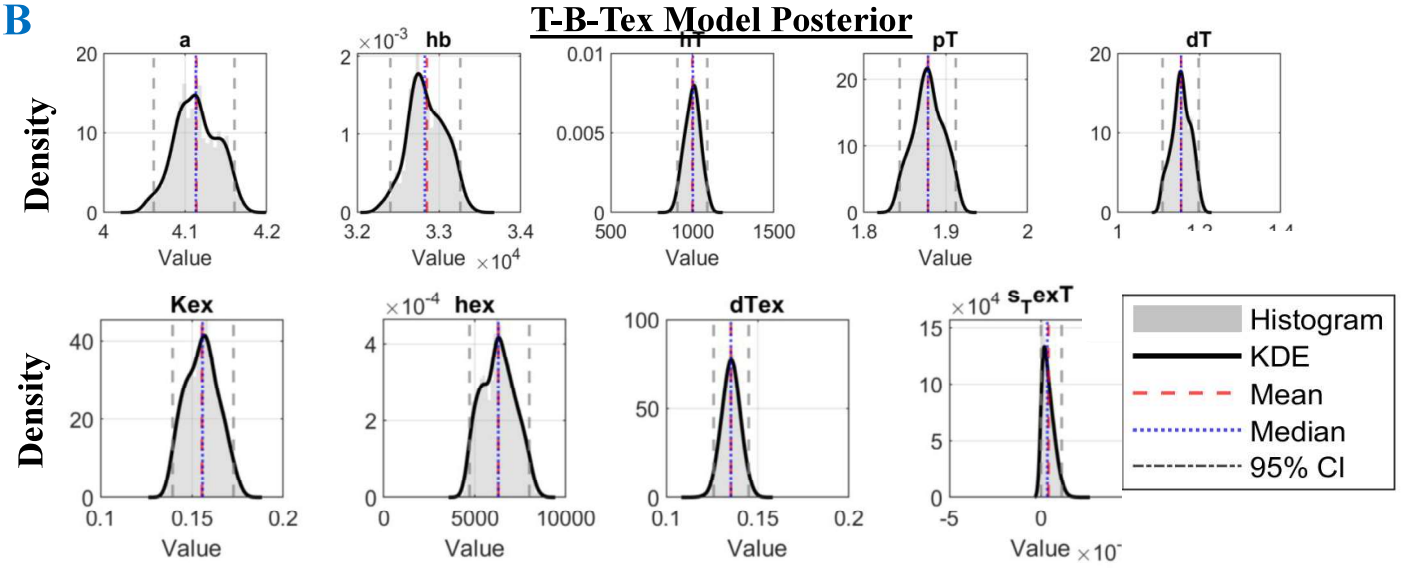

C

T-B-Tex Model Residual Analysis

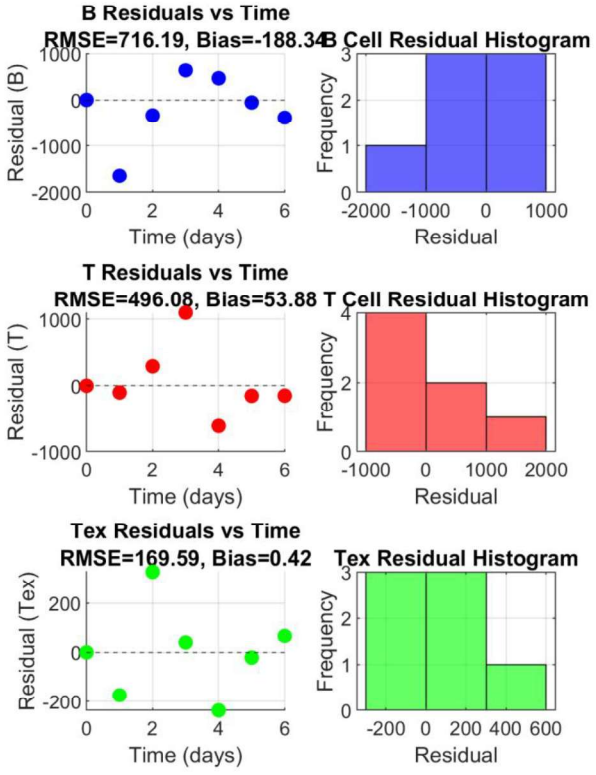

T-B-Tex Model	RMSE	Bias
B cells	716.19	-188.34
T cells	496.08	53.88
T_{ex} Cells	169.59	0.42

Figure S4:*Markov Chain Monte Carlo (MCMC) and residual analysis for model 2 parameter estimation. (A) Experimental setup for quantifying $CD19^+$ B cells, $CD8^+$ T cells, and $PD\text{-}1^+$ exhausted T cells in blinatumomab-treated co-cultures. Primary T cells and BV173 cells were plated at an effector-to-target ratio of 1:2 in round-bottom 96-well plates. Six independent replicates were monitored daily for six days by flow cytometry. Gating strategy is shown in Supplementary Figure S1C. (B) Overview of the mathematical modeling framework used to describe T–B dynamics. Model 1 incorporates logistic B-cell growth (r_B, K_B), T-cell-mediated B-cell killing (a, n_B, h_B), B-cell–dependent T-cell proliferation (p_T, n_T, h_T), and natural T-cell death (dT). Parameters were estimated by fitting the ODE model to experimental data using Markov Chain Monte Carlo (MCMC) methods. (C) MCMC parameter estimation results for Model 1. Trace plots show mixing and convergence of posterior samples. Posterior distributions are shown for all model parameters, illustrating parameter ranges and uncertainty. (D) Residual analysis for Model 1, comparing observed and simulated B-cell and T-cell counts over six days. Plots show residuals across all time points for both populations.

Figure S5

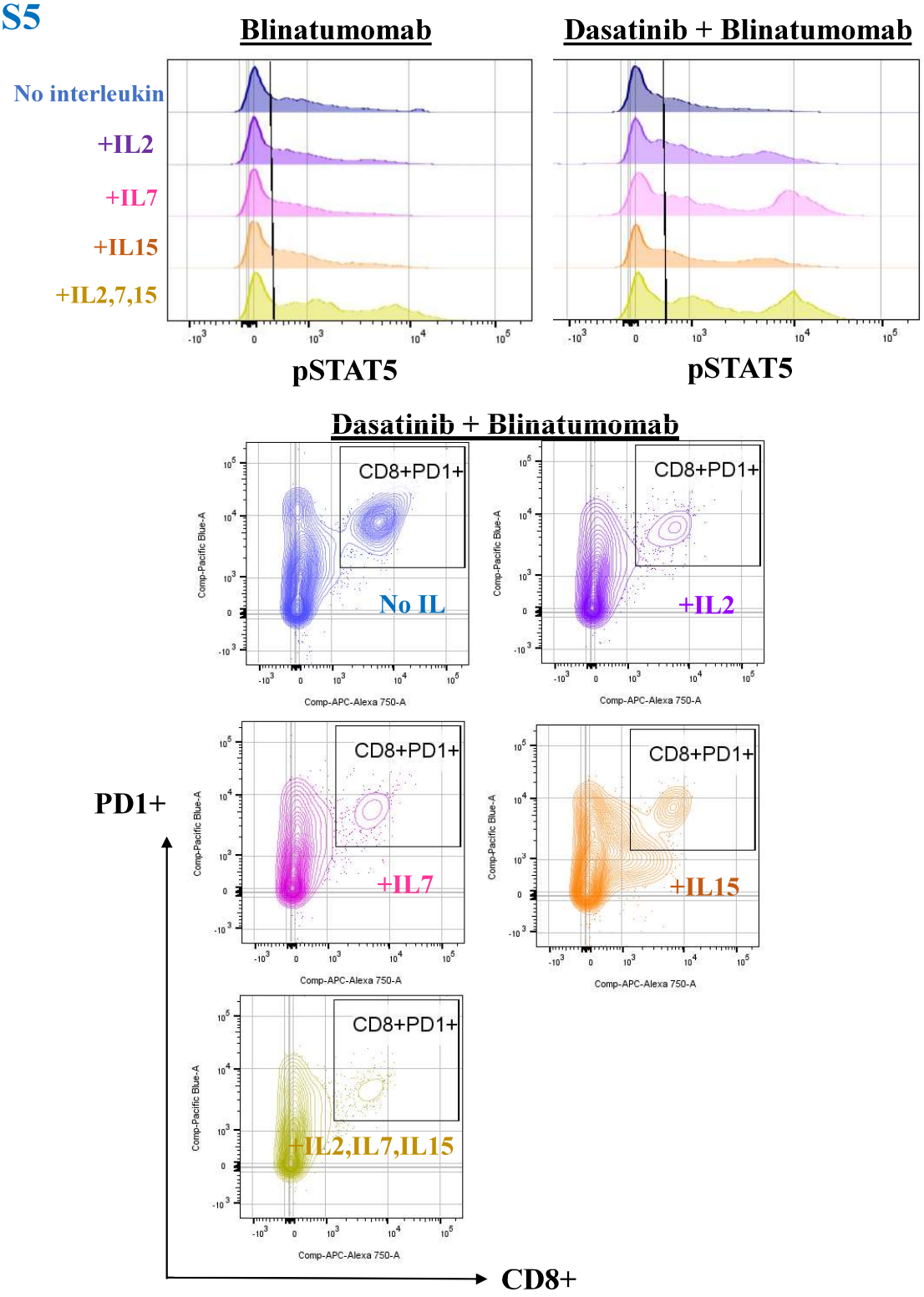

Figure S5:*Interleukins reverse the T cell exhaustion by Src/BCR-ABL TKIs through pstat5 signaling pathway. (A) Flow-cytometric analysis of intracellular pSTAT5 levels in T cells treated with blinatumomab alone or with interleukins (IL-2, IL-7, IL-15). Histograms show increased pSTAT5 following interleukin addition, both with blinatumomab alone and with blinatumomab plus dasatinib. (B) Gating of $CD8^+$ T cells and PD-1 expression for conditions shown in Figure 4. Flow plots show the percentage of $CD8^+$ $PD\text{-}1^+$ T-cells under dasatinib treatment, with interleukin addition partially reducing PD-1 expression.

Figure S6

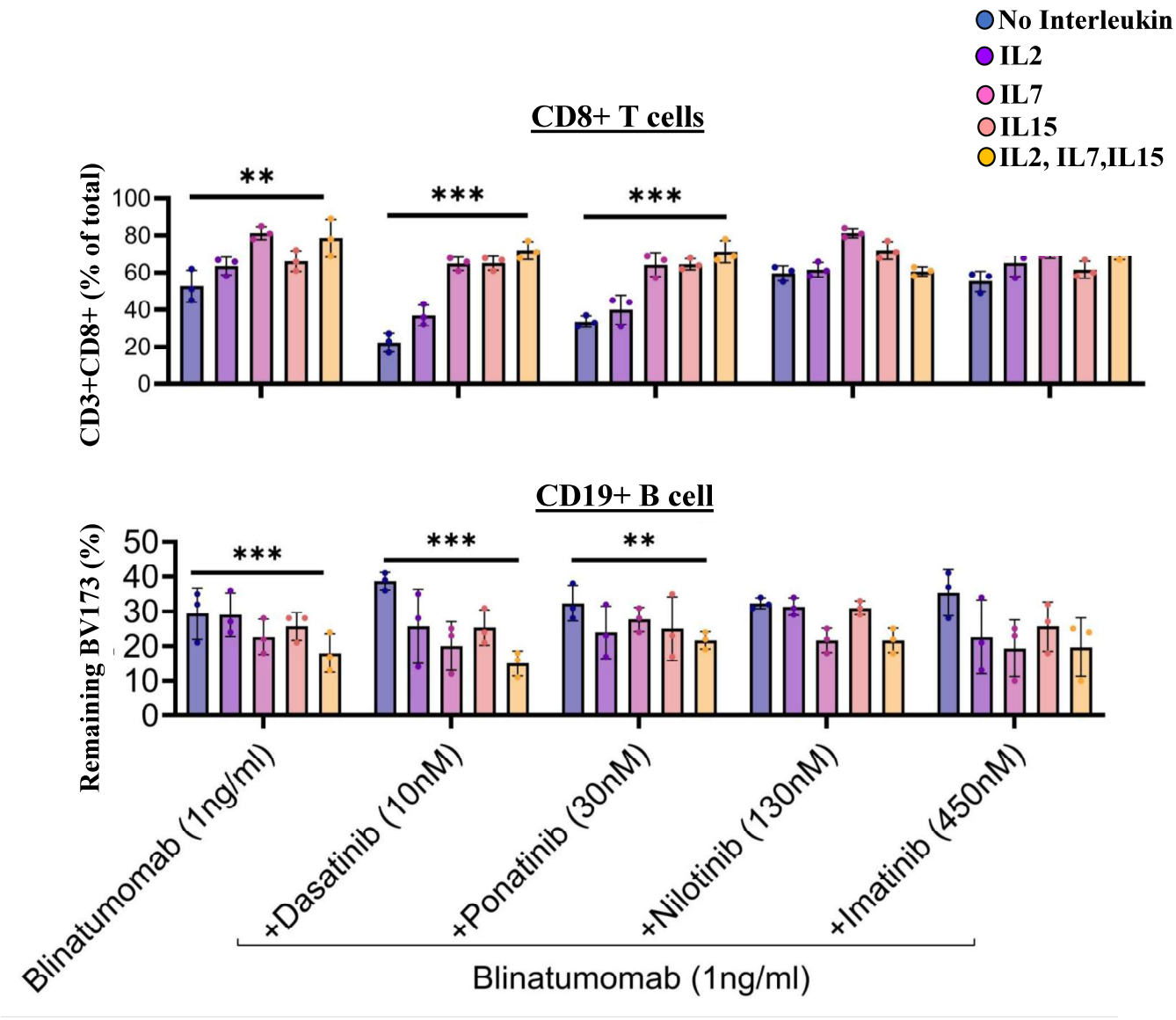

Figure S6:*Cytokines IL-2, IL-7, and IL-15 rescue the antagonistic effects of dual Src/BCR-ABL TKIs on Blinatumomab efficacy. Co-cultures of primary T cells and BV173 leukemia cells were treated for 48–72 hours with blinatumomab (1 ng/mL) alone or in combination with dual Src/BCR-ABL TKIs (dasatinib, ponatinib), BCR-ABL–selective TKIs (imatinib, nilotinib), and/or common γ-chain cytokines (IL-2, IL-7, IL-15; 10 ng/mL each). T-cell proliferation and BV173 cell clearance were quantified. Cytokine supplementation, particularly IL-7, restored T-cell expansion and enhanced blinatumomab-mediated leukemia cell killing in the presence of dual Src/BCR-ABL TKIs. Statistical significance was assessed using one-way ANOVA with Dunnett's post-hoc test comparing each treatment condition to blinatumomab alone. Significance thresholds: $P<0.05$ (*), $P<0.01$ (**), $P<0.001$ (***), $P<0.001$ (****), ns = not significant.